iMed

SCIEPublish

Review

From Physical Amplification to Biological Effect: The Evolving Landscape of Nucleic Acid Nanomedicines in Radio-Immunotherapy

Chuxuan Long [1,†], Yi Zhu [1,†], Namei Ji [1,†], Xiumei Ma [2,*], Chunlin Shao [3,*] and Yuexia Xie [1,*]

[1] Central Laboratory, Ren Ji Hospital, School of Medicine, Shanghai Jiao Tong University, No. 160 Pu-Jian Road, Shanghai 200127, China; longchuxuan@sjtu.edu.cn (C.L.); cecelia.juju@sjtu.edu.cn (Y.Z.); jnanam_430@sjtu.edu.cn (N.J.)

[2] Department of Radiation Oncology, Ren Ji Hospital, School of Medicine, Shanghai Jiao Tong University, No. 160 Pu-Jian Road, Shanghai 200127, China

[3] Institute of Radiation Medicine, Shanghai Medical College, Fudan University, No. 2094 Xie-Tu Road, Shanghai 200032, China

* Corresponding author. E-mail: maxiumei@renji.com (X.M.); clshao@shmu.edu.cn (C.S.); xieyuexia@sjtu.edu.cn (Y.X.)

† These authors contributed equally to this work.

Received: 26 May 2026; Revised: 9 June 2026; Accepted: 16 July 2026; Available online: 31 July 2026

ABSTRACT: Radiotherapy (RT) remains a mainstay of cancer treatment, but its efficacy is limited by radioresistance and immunosuppression. Nucleic acid therapeutics, including siRNA, microRNA modulators, antisense oligonucleotides, aptamers, CpG oligodeoxynucleotides, and CRISPR systems, can remodel tumor responses at multiple levels. Nanotechnology enables their precise delivery, protection, and spatiotemporal activation. This review synthesizes recent advances in nucleic acid-enabled radiosensitization across four dimensions: (1) precise delivery via passive/active targeting and radiation-triggered release; (2) target selection from dominant-node inhibition to coordinated network regulation; (3) immune remodeling from checkpoint blockade to active immune instruction; and (4) multimodal integration where RT serves as a biological switch. We formally define programmable radio-nanomedicine as the co-design of nucleic acid cargo, carrier logic, activation trigger, and radiation schedule so that irradiation acts as a context-defining event. Translational barriers and a framework for next-generation design are discussed.

Keywords: Radiotherapy; Radiosensitization; Nucleic acid nanomedicine; Tumor microenvironment; Radio-immunotherapy

1. Introduction

Radiotherapy (RT) is used in more than half of patients with cancer during the course of their disease [1–3]. It remains indispensable for local tumor control across a broad range of solid malignancies [4,5]. Its biological effects are conventionally understood through direct DNA ionization and indirect generation of reactive oxygen species (ROS), resulting in DNA double-strand breaks, mitotic catastrophe, apoptosis, senescence, vascular damage, and, in some settings, immunogenic cell death (ICD) [4–7]. Yet the clinical efficacy of RT is constrained by several persistent problems. First, many tumors exhibit intrinsic or adaptive

radioresistance driven by hypoxia, DNA repair activation, cell-cycle redistribution, anti-apoptotic signaling, metabolic rewiring, stemness programs, and invasive escape [8–11]. Second, dose escalation is limited by normal tissue toxicity. Third, although irradiation can prime immunity, it may also induce compensatory immunosuppression, including upregulation of PD-L1, recruitment of myeloid-derived suppressor cells (MDSCs), polarization of tumor-associated macrophages, and stromal remodeling that protects residual disease [12–15].

Beyond local control, RT optimization also aligns with the broader goal of improving the quality of life and well-being for patients with cancer. Dose escalation is often constrained by late toxicity, whereas many systemic combinations increase financial and biological burden. Nanomedicine-assisted radiosensitization may contribute to this clinical goal by improving tumor selectivity, reducing unnecessary normal-tissue exposure, and enabling lower or more rationally fractionated radiation doses. This perspective is consistent with the broader health-care objective embodied in Sustainable Development Goal 3—good health and well-being—because it links technological innovation with treatment accessibility, toxicity reduction, and durable functional outcomes [16,17].

Nucleic acid therapeutics have emerged as particularly well-suited to this challenge. Unlike conventional small molecules, which often act on a restricted set of protein classes, nucleic acid drugs can be designed against nearly any transcript or signaling hub. Small interfering RNA (siRNA) can silence radioresistance drivers; antisense oligonucleotides can inhibit oncogenic transcripts or splice variants; aptamers can function both as targeting ligands and checkpoint antagonists; CpG oligonucleotides can act as immune adjuvants; and CRISPR systems can be deployed to identify or disrupt synthetic-lethal genes linked to radiation response [18–23]. These tools are especially attractive in radiobiology, where resistance is rarely strictly monogenic but is often organized around a limited number of pathway nodes—DNA repair, antioxidant defense, hypoxia response, ferroptosis suppression, immune escape, and migration/invasion. In principle, nucleic acids enable precise, modular intervention at each of these levels [24–26].

The central obstacle is delivery. Free nucleic acids are unstable in circulation, prone to nuclease degradation, poorly permeable across cell membranes, inefficient at crossing barriers such as the blood-brain barrier (BBB), and susceptible to rapid clearance and off-target distribution [18,27]. Nanomedicine addresses these limitations by protecting cargo, prolonging circulation, enabling tumor accumulation, incorporating cell-specific ligands, and allowing intracellular release [28–35]. Increasingly, these platforms are not just passive carriers but programmable systems: they can respond to hypoxia, ATP, MMP-2, ROS, pH, or even the radiation event itself [36–40]. In this sense, RT is no longer just the therapeutic partner. It becomes a biological switch that can change nanoparticle behavior, trigger cargo release, amplify DNA damage, expose antigens, or selectively create the conditions required for a second immune-activating step.

For conceptual clarity, we define programmable radio-nanomedicine as a nanoscale therapeutic system in which the nucleic acid cargo, carrier architecture, activation trigger, and radiation schedule are deliberately co-designed so that irradiation acts as a spatially and temporally defined biological input. This concept differs from conventional stimuli-responsive nanocarriers, which usually respond to a pre-existing tumor feature such as pH, glutathione, hypoxia, or an enzyme. In programmable radio-nanomedicine, the radiation beam itself creates or amplifies the trigger (ROS, ATP, MMP-2, PD-L1 induction, DNA damage, or ICD), thereby linking therapeutic activation to the treatment field and schedule.

Recent papers in this area reveal an important conceptual transition. Earlier work often treated radiosensitization as a local cytotoxic problem: deliver a nucleic acid, inhibit one resistance factor, and improve clonogenic kill. Newer studies ask how one should deliver, what kind of target architecture should be selected, how the irradiated tumor immune ecosystem should be remodeled, and how multiple modalities can be coordinated in time and space. These questions define the structure of the present review.

The perspective advanced here is that the field is best understood across four interlocking dimensions (Figure 1). The first is precise delivery, encompassing passive accumulation, active receptor targeting,

barrier penetration, membrane fusion, and irradiation-triggered local release. The second is the target architecture, namely the strategic choice between dominant-node inhibition and coordinated regulation of several resistance mechanisms. The third is immune remodeling, which has evolved from simply blocking inhibitory pathways toward active immune instruction through adjuvants, dendritic-cell activation, and memory formation. The fourth is the multimodal joint model, in which RT, photothermal therapy, checkpoint blockade, ferroptosis induction, hypoxia modulation, and nucleic acid programming are combined into synchronized systems.

This framework also offers a way to move beyond existing reviews. Rather than organizing the field only by cargo type or nanoparticle material, it places emphasis on the logic of therapeutic programming. This shift is important because clinically meaningful radiosensitization will likely depend less on finding the single "best" nanoparticle and more on designing systems in which cargo, carrier, radiation schedule, and tumor ecology are biologically aligned.

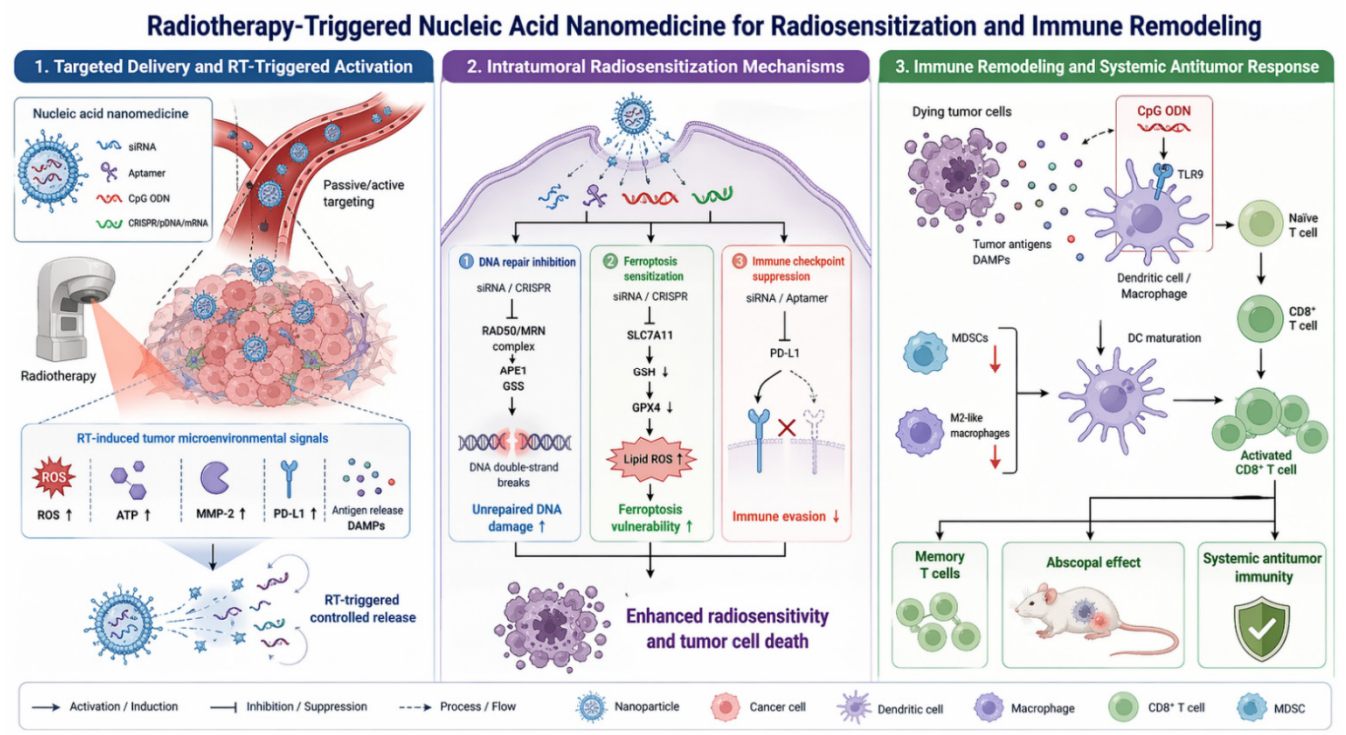

Figure 1. Schematic overview of radiotherapy-triggered nucleic acid nanomedicine for radiosensitization and systemic immune remodeling. The platform integrates three coordinated modules. (1) Targeted delivery and RT-triggered activation: Nucleic acid therapeutics (siRNA, aptamers, CpG ODNs, and CRISPR/pDNA/mRNA) are delivered to the tumor and undergo controlled release in response to radiotherapy-induced microenvironmental signals, including elevated ROS, ATP, MMP-2, and PD-L1; (2) Intratumoral radiosensitization: Nucleic acid cargoes inhibit DNA repair pathways (e.g., RAD50/MRN complex, APE1, GSS), amplify unrepaired DNA damage, and sensitize tumor cells to ferroptosis by suppressing the SLC7A11/GPX4 axis and promoting lipid peroxidation, thereby enhancing overall radiosensitivity and tumor cell death; (3) Immune remodeling and systemic antitumor response: Radiotherapy-induced immunogenic cell death releases tumor antigens and DAMPs; CpG ODNs engage TLR9 on dendritic cells and macrophages to promote DC maturation and $CD8^+$ T-cell activation. Concomitant repolarization of M2-like macrophages and reduction of MDSCs facilitate the generation of memory T cells and abscopal effects, establishing durable systemic antitumor immunity.

2. The Arsenal and the Battlefield—Nucleic Acid Drugs and the Mechanisms of Radiosensitization

2.1. The Arsenal: A Guide to Nucleic Acid Therapeutics

Nucleic acid drugs are molecular instructions. Unlike traditional small-molecule drugs that mostly interfere with proteins, these therapies work at the genetic level, instructing the cell to change its behavior

[41]. The diversity of this arsenal has expanded rapidly, offering a range of tools from precise molecular scalpels to broad-spectrum regulators.

2.1.1. Gene Silencing Tools

The most precise instruments in our arsenal are those designed for gene silencing. For years, the workhorse of this approach has been small interfering RNA (siRNA). These short, double-stranded RNA molecules hijack a cell's own powerful machinery, the RNA-induced silencing complex (RISC), to seek out and destroy specific messenger RNAs (mRNAs), effectively preventing the production of a targeted protein [42–46]. It is a remarkably efficient system, and its potential for cancer therapy was demonstrated early on by using nanoparticles to deliver siRNA against the DNA repair protein Ape1, successfully sensitizing resistant cancer cells to radiation [47]. However, siRNA relies on the cell's endogenous machinery, which can be a limitation. A more self-sufficient tool is the DNAzyme. These are synthetic, single-stranded DNA molecules with catalytic activity. They bind to a specific mRNA sequence and, in the presence of a cofactor like magnesium, directly cleave it, acting as a true, self-contained enzyme [48]. This independence makes DNAzymes an attractive option for targeting genes in situations where the cellular machinery might be compromised.

Moving from single-gene scalpels to broader regulators, we encounter microRNA (miRNA) and long non-coding RNA (lncRNA). Unlike siRNA, which typically silences one specific gene, a single miRNA can bind to and regulate the expression of hundreds of different mRNAs, making it a master switch that can rewire entire cellular networks [49,50]. This makes miRNAs particularly attractive for tackling complex phenotypes like cancer stemness or metastasis, but it also increases the risk of off-target effects. For this reason, the field has moved towards using combinations of miRNA mimics or inhibitors to achieve a more controlled, synergistic effect. Long non-coding RNAs, on the other hand, are a more recently appreciated class of regulators. These lengthy RNA molecules do not code for proteins but instead act as central hubs, orchestrating gene expression at the chromatin, transcriptional, and post-transcriptional levels. Targeting a single oncogenic lncRNA, such as MNX1-AS1, can therefore disrupt an entire pro-survival signaling pathway, offering a powerful "upstream" intervention point that simultaneously affects multiple downstream effectors [51].

2.1.2. Gene Overexpression Tools

Beyond silencing, there are situations in which we want to restore or enhance the function of a gene. This is the domain of gene overexpression tools. Plasmid DNA (pDNA) is the classic tool for this purpose. These are circular DNA molecules engineered to carry a therapeutic gene that, once delivered into the nucleus of a cell, can be transcribed into mRNA and translated into a functional protein [52,53]. However, the requirement for nuclear entry is a significant delivery hurdle. An alternative that has gained tremendous momentum is messenger RNA (mRNA) itself. *In vitro*-transcribed mRNA acts directly in the cytoplasm, where it is translated into protein, completely bypassing the need for nuclear entry and eliminating the risk of insertional mutagenesis, a safety concern with DNA-based approaches [54–57]. This makes mRNA a particularly attractive platform for applications like tumor suppressor replacement or cancer vaccine development.

2.1.3. Immune Modulation Tools

A powerful category of nucleic acid drugs doesn't target cancer cells directly but instead engineers the immune system. CpG oligodeoxynucleotides (CpG ODNs) are short DNA sequences that mimic bacterial DNA [58–60]. They are recognized by Toll-like receptor 9 (TLR9) on immune cells like dendritic cells and macrophages, acting as a potent danger signal that jolts these cells into action, transforming a "cold", immunosuppressive tumor environment into a "hot", inflamed one [61–65]. Another versatile tool is the

nucleic acid aptamer. These are short, single-stranded DNA or RNA molecules that fold into unique three-dimensional shapes, allowing them to bind to specific target proteins with an affinity rivaling that of antibodies [66–68]. Aptamers can be used as "homing devices" to guide nanoparticles to cancer cells, or they can themselves act as therapeutic agents by blocking protein-protein interactions, such as the PD-1/PD-L1 immune checkpoint [69–72]. With this diverse arsenal in hand, we now turn to the challenge of understanding the enemy's defenses.

2.2. The Battlefield: Unpacking the Mechanisms of Radiosensitization

To understand how nucleic acid drugs boost radiation sensitization, one must first consider the sophisticated, multilayered defenses that cancer cells have against them. Radiotherapy exerts its primary effect by inducing DNA damage, yet the cancer cell's response is far from passive—it constitutes a coordinated counterattack [73].

2.2.1. Targeting the DNA Damage Repair System

The DDR system is one of the most direct defenses against ionizing radiation. DSBs are mainly repaired by HR and NHEJ, with the MRN complex, DNA-PKcs, RAD50, APE1, and PARP-related pathways providing therapeutically exploitable nodes [74–80]. Early nanoparticle-delivered siApe1 studies showed that suppressing the BER pathway can sensitize glioblastoma cells to radiation [47], but subsequent work highlighted the activation of compensatory repair. More recent designs, therefore, target broader repair hubs or couple repair blockade with immune regulation. For example, siRAD50 delivered by polymer-lipid nanoparticles disrupted the MRN complex and reduced the radiation dose required for 50% colony formation in triple-negative breast cancer cells [81]. BNCT combined with PD-L1 siRNA further illustrates cross-module targeting: boron-mediated high-linear-energy-transfer damage increased DSBs, while PD-L1 silencing reduced BRCA1, MRE11, and RAD50-associated repair support and relieved immune escape [82]. Thus, DDR targeting is most powerful when repair inhibition is integrated with redox or immune programs rather than treated as an isolated single-protein intervention.

2.2.2. Regulating Cell Cycle Checkpoints

Cell-cycle checkpoints provide the temporal window needed for repair. ATM/ATR-Chk1/Chk2 signaling pauses progression after radiation-induced damage [83–85]. A representative nucleic-acid strategy is FBXW7 DNAzyme therapy. By preventing FBXW7-mediated degradation of phosphorylated p53, the DNAzyme-Fe nanoassembly stabilized p53, enforced G2 arrest, and simultaneously suppressed the SLC7A11/GSH/GPX4 anti-ferroptosis axis [48]. This design shows how a nominally single genetic node can regulate multiple resistance modules—checkpoint recovery, apoptosis commitment, and ferroptosis sensitivity—when selected based on pathway topology.

FBXW7 further illustrates why checkpoint control should be viewed as a dynamic decision node rather than a static arrest signal. Although FBXW7 is classically recognized as a tumor-suppressive E3 ubiquitin ligase whose loss-of-function is clinically significant across human cancers, DNA damage and repair biomarkers also shape immunotherapy response and the broader clinical translation of DDR-targeted therapy [86–88]. In the radiotherapy setting, this literature supports the interpretation that FBXW7-dependent regulation of phosphorylated p53 can influence whether irradiated cells pause for repair, recover from checkpoint arrest, or proceed toward irreversible arrest and death. Therefore, combining FBXW7 manipulation with the DNAzyme-Fe nanoassembly provides a biologically coherent checkpoint-redox strategy rather than an isolated ferroptosis intervention [48].

2.2.3. Overcoming Apoptosis Evasion and Inducing Specific Cell Death Pathways

If DNA damage is too severe, the cell can still escape death by blocking its own internal self-destruct sequence, triggering a process known as apoptosis evasion [89,90]. This is often achieved by tipping the balance of the Bcl-2 family of proteins towards survival, upregulating anti-apoptotic members like Bcl-2 and Bcl-xL, or downregulating pro-apoptotic ones like Bax [91–94]. More recently, a completely different cell death pathway has come into focus: ferroptosis. This iron-dependent form of cell death is driven by the catastrophic peroxidation of lipids in the cell membrane [95–97]. Radiotherapy itself can trigger ferroptosis by generating reactive oxygen species (ROS) [76,98]. However, cancer cells have robust defense systems centered on the SLC7A11/GSH/GPX4 axis that neutralize these lipid peroxides [8]. It is discovered that p53, the same protein involved in cell cycle arrest, also transcriptionally suppresses SLC7A11, creating a powerful link between apoptosis and ferroptosis. This suggests that a well-chosen single target, such as p53, can exert a synergistic effect by promoting cell cycle arrest and sensitizing the cell to ferroptosis [99,100]. Furthermore, the strategic use of metal ions can directly amplify ferroptosis. For instance, Fe^{3+} ions can consume intracellular glutathione (GSH), breaking down the cell's antioxidant shield and preserving the ROS generated by radiation. At the same time, Fe^{2+} catalyzes the Fenton reaction, producing highly toxic hydroxyl radicals [101].

2.2.4. Remodeling the Tumor Microenvironment

The tumor microenvironment (TME) adds another layer of resistance. Hypoxia reduces oxygen fixation of DNA damage, while HIF signaling promotes survival, invasion, stemness, and immune suppression [102–108]. Cancer-associated fibroblasts (CAFs) can support tumor growth, remodel extracellular matrix, and suppress immune attack; recent studies further indicate that CAF metabolic reprogramming and signaling pathways can be therapeutically targeted or re-educated [109,110]. Stromal and immune cells can either protect residual disease or be reprogrammed into therapeutic allies. For example, PD-L2-targeted fluorinated PEI nanoparticles carrying an aPD-L1-P2A-CD86 plasmid converted immunosuppressive CAFs into antigen-presenting, antibody-secreting cells after RT, avoiding destructive CAF depletion while enhancing memory T-cell generation [111]. Conversely, low-dose RT can increase M2-like macrophages and MDSCs unless paired with immune adjuvants; DNA nanoclusters co-delivering CpG reversed this myeloid shift and strengthened systemic antitumor immunity [112]. Therefore, successful radio-nanomedicine should actively remodel the TME instead of assuming it is a passive delivery space.

2.2.5. Intervening in Metabolic Reprogramming

To fuel their relentless growth and repair efforts, cancer cells undergo a profound metabolic reprogramming. A key aspect of this is enhanced fatty acid oxidation (FAO), which provides energy in the form of ATP and also supplies carbon backbones for membrane synthesis and signaling molecules [113]. In glioblastoma, it was discovered that FAO fuels radioresistance and, through a citrate-acetyl-CoA-RelA pathway, upregulates the "don't eat me" signal CD47, allowing cancer cells to evade macrophage attack. The combination of an FAO inhibitor and an anti-CD47 antibody significantly improved treatment outcomes in a mouse model of recurrent glioblastoma [114]. Beyond lipid metabolism, high expression of glutamine synthetase has been linked to enhanced DNA repair and radiation resistance, while increased purine levels directly provide the building blocks for repairing damaged DNA [73]. Targeting these metabolic vulnerabilities offers another avenue for radiosensitization.

2.2.6. Targeting Cancer Stem Cell Programs

Finally, lurking within the tumor are small subpopulations of cells with an outsized capacity for resistance and regeneration. These cancer stem cells (CSCs) are often intrinsically more radioresistant than

the bulk of the tumor. They typically have more efficient DNA repair systems, such as higher expression of RAD51, lower levels of reactive oxygen species (ROS) due to enhanced scavenging systems, and can reside in a quiescent, radioresistant G0 phase of the cell cycle [115]. Therefore, effective radiosensitization must also target this resilient population. Strategies include directly targeting their unique DNA repair pathways, using agents that amplify ROS to overwhelm their antioxidant defenses, or using differentiation therapy to push CSCs out of their resistant stem-like state and into a more vulnerable, differentiated state [116]. The combination of all these strategies—disrupting DNA repair, manipulating cell cycle checkpoints, inducing cell death, and dismantling the protective TME—represents the modern, holistic approach to making radiation a truly curative therapy [117].

2.2.7. Mechanistic Cross-Talk: DNA Damage, Ferroptosis, ICD, and Antitumor Immunity

Nucleic acid radiosensitization is best understood as a set of coupled biological circuits rather than a sequence of independent effects. Radiation first induces DSBs and ROS; siRNA, DNAzyme, antisense, or CRISPR interventions can prolong this damage by suppressing DDR or antioxidant nodes. If redox pressure is redirected toward lipid peroxidation, the same radiation event can also drive ferroptosis through the SLC7A11/GSH/GPX4 axis [8,48,95–101]. Ferroptosis and apoptosis-resistant death then feed into ICD by promoting exposure or release of calreticulin, HMGB1, ATP, tumor antigens, and nucleic acid fragments, which engage TLR9- and cGAS/STING-related innate sensing pathways. Whether this converts into durable immunity depends on the downstream immune context: CpG or STING activation can mature dendritic cells and induce type I interferon, whereas PD-L1, MDSCs, Tregs, and M2 macrophages can terminate the response [82,112,118–121]. This cross-talk explains why combination designs that coordinate DDR inhibition, ferroptosis induction, and immune instruction often outperform designs that amplify only one physical or biochemical event.

To improve comparability across studies, Table 1 should be interpreted using several minimal reporting elements: radiation modality and energy, total dose and fractionation, dose rate when available, sequence and route of nanomedicine administration, tumor model and immune competence, primary radiosensitization endpoint (e.g., SER at a specified surviving fraction), and systemic endpoints such as distant-lesion response or memory rechallenge. Whenever these parameters are not reported, the apparent magnitude of radiosensitization or abscopal activity should be interpreted cautiously.

The nucleic acid drug types and radiosensitization mechanisms discussed in the above subsections have been validated by various nanoplatforms. Table 1 summarizes representative nucleic acid-loaded nanoradiosensitizers reported in recent years, including their radiation parameters, composition, targeting strategies, nucleic acid types, and core mechanisms. It serves as a reference linking the theoretical concepts in Section 2 to concrete examples.

Table 1. Comprehensive Summary of Nucleic Acid-Loaded Nanoradiosensitizers and Their Key Characteristics.

Year	Radiation Characteristics	Mechanism	Composition Details	Target Ways	Loaded Nucleic Acid Type and Sequence
2022 [122]	6 MV X-ray, (0–8 Gy)	↑ cellular uptake via clathrin-mediated endocytosis ↑ ROS, SER = 1.62	PEGylated Ag@Au core-shell nanoparticles (11 nm)	Active targeting (GMT8 aptamer)	DNA 5′-TGACGAGCCCAAGTTACCTCGTACTTGTGTGTTTAATTGTTTATTGCTGTCACGTGAGAATCTCCGCTGCTACTA-3′, 5′-$(CH_2)_6$-NH_2
2023 [123]	X-ray, 3 fractions (8 Gy)	↓ EGFR and IKKα, ↓ NF-κB, ↓ DNA repair, ↑ survival	Bacteriophage Qβ VLPs with b-3WJ RNA scaffold (30 nm)	Active targeting (ApoE/TAT) + Coordinated Regulation	RNA (siRNA + miRNA) siRNA (EGFR) + miRNA Let-7g
2017 [47]	Fractionated (2–10 Gy)	↓ Ape1 (BER pathway), ↑ γ-H2AX, ↑ radiosensitization	Iron oxide core, chitosan-PEG-PEI copolymer, chlorotoxin targeting (48.5 nm)	Active targeting (chlorotoxin) + Single Attack	siRNA siApe1 (SMARTpool)
2024 [81]	X-ray (10 Gy)	↓ RAD50, ↓ DNA repair (HR), ↑ γ-H2AX, ↑ apoptosis	Polymer-lipid hybrid nanoparticles (102–118 nm)	Active targeting (intratumoral injection) + Single Attack	siRNA siRAD50
2025 [82]	BNCT (neutron) + 2 Gy ×2	↓ PD-L1, ↓ BRCA1/RAD50, ↑ DNA damage, ↑ ICD, ↑ T cell immunity	Boron-containing polymer self-assembled with PD-L1 siRNA, disulfide-crosslinked (97 nm)	Active targeting (cRGD) + Coordinated Regulation (PD-L1 + DNA repair)	siRNA siPD-L1
2021 [118]	X-ray (2 Gy, 4 fractions)	ATP-responsive release of CpG from alginate-based hydrogel; RT induces ICD → ATP burst → competitive binding releases CpG; ↑ DC maturation, ↑ $CD8^+$ T cells, abscopal effect	Alginate hydrogel conjugated with ATP-specific aptamer (Aapt), hybridized with CpG-cAptamer; Ca^{2+}-induced gelation *in situ*	Active Activation (CpG as adjuvant) + Radiation as delivery gate (ATP released by RT)	DNA CpG-cAptamer: CpG sequence (TCCATGACGTTCCTGACGTT) extended with 16 bases complementary to Aapt; ATP Aptamer-NH_2: NH_2-ACCTGGGGGAGTATTGCGGAGGAAGGT
2024 [39]	X-ray (6 Gy) + 808 nm laser (PTT)	↑ ROS, ↑ ICD, ↑ DC maturation, ↑ $CD8^+$ T cells, ↓ M2 macrophages	Gold-MnO_2 nanoflowers (72.5 nm) conjugated with PD-L1 aptamer	Active targeting (PD-L1 aptamer) + Multimodal (RT+PTT+ICB)	DNA PD-L1 aptamer (sequence NR)

2022 [124]	X-ray (priming dose 4 Gy) + second RT	Two-step RT: first dose recruits macrophages → vascular bursts → 25-fold enhanced AuNP-CpG accumulation; M2→M1 repolarization; second RT sensitized; αPD-L1 synergy	AuNPs (13 nm) conjugated with thiolated CpG (AuNPs-CpG); spherical nucleic acids (SNAs)	Passive (EPR) + Radiation as delivery gate (macrophage recruitment) + Coordinated Regulation (radiosensitization + immune adjuvant)	DNA 5′-SH-AAAAAAAATCCATGACGTTCCGAGTT-3′
2018 [125]	6 MV X-ray (megavoltage)	AS1411 aptamer targets nucleolin; BSA-GNCs as radiosensitizer; DEF = 2.7 (clonogenic)	BSA-coated gold nanoclusters (GNCs, ~7.7 nm) conjugated with AS1411 aptamer	Active targeting (AS1411 aptamer to nucleolin) + Single Attack	DNA AS1411 aptamer (sequence: 5′-GGTGGTGGTGGTTGTGGTGGTGGTGG-3′)
2021 [126]	4 MV electron beam (0–6 Gy)	↑ Au uptake, ↑ apoptosis, SER = 1.66 (MDA-MB-231), 1.91 (mammosphere)	AS1411-conjugated gold nanoparticles (10 nm)	Active targeting (AS1411) + Single Attack	DNA 5′-GGTGGTGGTGGTTGTGGTGGTGGTGGTTTT-SH-3′
2023 [36]	X-ray (2–8 Gy)	↓ CFL1, ↓ invasion, ↑ DNA damage, ↑ radiosensitization	Selenium-engineered mesoporous silica nanocapsules (SeMSN, ~110 nm) with hypoxia-responsive P(MNs) coating and Angiopep-2 targeting	Active targeting (Angiopep-2) + Radiation as delivery gate (ROS-triggered Se-Se cleavage) + Coordinated Regulation	siRNA siCFL1
2023 [127]	X-ray (6 Gy)	↓ PGK1, ↓ ATP production, ↑ chemo/radiosensitivity	Biomimetic hypoxia-triggered RNAi nanomedicine (poly(MIs)/PTX@PEI/siPGK1@CCM, 107 nm)	Active targeting (cancer cell membrane homing) + Radiation as delivery gate (hypoxia-triggered) + Coordinated Regulation	siRNA siPGK1
2023 [112]	X-ray (5 Gy)	↑ ROS, ↑ CRT/HMGB1/ATP, ↑ DC maturation, ↑ abscopal effect	DNA nanoclusters (DNAnc, 256.9 nm) self-assembled from Y-shaped CpG-ODN-loaded DNA vectors	Passive (EPR) + Active Activation (CpG as adjuvant) + Multimodal (RT+immunotherapy)	DNA CpG ODN (extended sequence)
2022 [128]	X-ray (8 Gy)	High-Z Hf enhances RT, CpG activates DCs, ↑ abscopal effect, long-term immune memory	Hf-CpG MXF (metal-organic framework, ~90 nm)	Passive (EPR) + Active Activation (CpG) + Multimodal (RT + immunotherapy)	DNA CpG ODN (sequence NR)
2025 [129]	SABR (6 Gy ×3)	↓ Gal-1, ↑ ROS, ↑ γ-H2AX, ↑ DC, ↑ $CD8^+$ T cells, ↓ MDSC/Treg	Gold-siRNA supraclusters (BSCgal, 128 nm)—gold nanoclusters crosslinked with siRNA via DTSSP in PEG-amine matrix	Passive (EPR) + Active targeting (siRNA against Gal-1) + Coordinated Regulation	DNA/RNA CpG ODN 1826 (sequence NR) siGal-1

2026 [111]	X-ray (8 Gy)	↓ PD-L2 on CAFs, ↑ CD86, ↑ aPD-L1 secretion, ↑ T cell activation, prevents recurrence	PF_9PEI@aPC NPs (203 nm)—PD-L2-targeting peptide-modified PEI, loaded with aPD-L1-P2A-CD86 plasmid	Active targeting (PD-L2 peptide) + Relieving Inhibition (PD-L2 blockade) + Coordinated Regulation	DNA (plasmid) aPD-L1-P2A-CD86 plasmid
2024 [38]	X-ray (4 Gy)	↑ ATP, ↑ MMP-2, AND-gate release of eCpG, ↑ DC, ↑ T cell, ↑ systemic immunity	Fusogenic liposomes (Lip@AUR-ACP-aptPD-L1, 130 nm)	Active targeting (PD-L1 aptamer) + Radiation as delivery gate + Coordinated Regulation	RNA/DNA eCpG (CpG with aptATP-binding extension)
2025 [40]	X-ray (4 Gy)	↑ ROS, ↑ ICD, ↑ DC, ↑ $CD8^+$ T cells, ↓ MDSC, ↓ Treg	T cell membrane fusion liposomes (CIFL, 100 nm) loaded with Cy-I (iodine-containing cyanine) and CpG	Active targeting (PD-1/PD-L1 interaction) + Coordinated Regulation	DNA CpG ODN
2025 [130]	6 MV X-ray (0–8 Gy)	↑ DNA damage, ↑ apoptosis, SER = 1.34–1.63	PEGylated Ag@Au core-shell nanoparticles (13 nm) functionalized with TfRA4 and/or DNA1 aptamers	Active targeting (TfRA4 for BBB, DNA1 for GBM) + Single Attack	DNA TfRA4, DNA1 aptamers
2026 [131]	X-ray (4–8 Gy)	↑ ROS, ↑ γ-H2AX, ↑ DNA damage, SER = 1.27–1.69, ↓ IL-6/JAK2/STAT3	DNA-templated silver nanoclusters (NC-T5-5TR1, 2.85 nm) conjugated with 5TR1 aptamer	Active targeting (5TR1 aptamer to MUC1) + Single Attack + Signaling modulation	DNA 5TR1 aptamer (sequence: 5′-CCCCCCCCCCCTTTTTGAAGTGAA GATAGACAGAACACAACAC-3′)
2018 [132]	X-ray (4 Gy)	↑ STAT3 decoy, ↓ STAT3, ↑ DNA damage (γ-H2AX), ↑ apoptosis	Gold nanoparticles (13 nm) conjugated with NUAP aptamer and STAT3 decoy (STAT3d)	Active targeting (NUAP aptamer to nucleolin) + Coordinated Regulation	DNA (decoy) STAT3 decoy (sense: 5′-C* A* T* TTCCCGTAAATCTTT-3′, with thiol)
2023 [101]	X-ray (4 Gy)	↑ ATO (mitochondrial inhibition) + Fe^{3+} (GSH depletion), ↑ free radicals, ↑ radiosensitivity	Core: ATO@PAE-PEG; Shell: AS1411/Fe^{3+}	Active targeting (AS1411 aptamer) + Coordinated Regulation	DNA AS1411 aptamer (sequence: 5′-GGTGGTGGTGGTTGTTGGTGGTGG TGG-3′)
2023 [133]	NIR-II imaging + X-ray	↑ tumor retention (TBR = 7.97), ↑ ROS, ↑ radiosensitization	Degradable hafnium oxide core with ICG shell, PD-L1 aptamer-functionalized (Hf@ICG-Apt)	Active targeting (PD-L1 aptamer) + Multimodal (imaging+RT)	DNA PD-L1 aptamer (sequence: ACGGGCCACATCAACTCATTGATA GACAATGCGTCACTGCCGCT-NH_2)
2025 [134]	X-ray (6 Gy)	ATP-triggered aptamer assembly, PD-1/PD-L1 bispecific T cell engager, ↑ T cell killing	Cisplatin-loaded liposomes with X-ray-actuatable PD-L1/PD-1 bispecific aptamer precursors (Lip-cRGD@pCA@CIS)	Active targeting (cRGD) + Radiation as delivery gate + Coordinated Regulation	RNA aptPD-L1A, aptPD-1A (split ATP aptamer)
2025 [119]	X-ray (4 Gy)	↑ CRT, ↑ HMGB1, ↑ ATP, ↑ ICD, ↑ DC maturation, ↑ $CD8^+$ T cells, ↑ long-term memory	Metformin-based chitosan-siTREX1 nanocomplex (CSMT, 133 nm)	Active targeting (biguanide modification) + Coordinated Regulation	siRNA siTREX1

2025 [135]	X-ray (6 Gy)	↓ TRF2 (telomere deprotection), ↑ γ-H2AX, ↑ radiosensitivity, SER = 2.3	Peptide-gold nanoclusters (AuSGR2, 2.3 nm) complexed with siRNATRF2 (self-assembled ~110 nm)	Active targeting (positive charge, arginine-rich peptide) + Single Attack	siRNA siRNATRF2 (sequence: 5′-CCUUCUUUAGUGGUUUGCUUAUT T-3′)
2023 [48]	X-ray (8 Gy)	↓ FBXW7 via DNAzyme, ↑ p53, G2 arrest, ↓ SLC7A11, ↑ ferroptosis (Fe^{2+})	Coordination-driven DNAzyme-Fe nanoassembly with HA-DA coating (DNAzyme-Fe-HA, ~200 nm)	Active targeting (HA-CD44) + Coordinated Regulation (cell cycle + ferroptosis)	DNA FBXW7 DNAzyme (10-23 catalytic domain)
2023 [23]	X-ray (12 Gy)	↓ GSS via CRISPR/Cas9, ↓ GSH, ↑ ferroptosis	Engineered extracellular vesicles (EVs, 125 nm) with Angiopep-2 and TAT peptides, loaded with Cas9/sgRNA	Active targeting (Angiopep-2 for BBB, TAT for penetration) + Single Attack (gene editing)	RNA (sgRNA + Cas9 mRNA) sgRNA targeting GSS
2024 [136]	X-ray (6 Gy)	↓ circADARB1, ↓ HSP90B1, ↓ SLC7A11/GPX4, ↑ ferroptosis	Biomimetic semiconducting polymer nanoparticles (Fe@Pdots-siRNA, ~140 nm) coated with cancer cell membrane, loaded with iron and siRNA	Active targeting (cancer cell membrane homing) + Coordinated Regulation (circRNA + ferroptosis)	siRNA si-circADARB1
2026 [51]	X-ray (4 Gy)	↓ lncMNX1-AS1, ↓ Trop2, ↓ JAK3/STAT3, ↓ GSH, ↑ ROS, SER = 1.69	TNBC-targeted reduction-responsive RNAi nanoplatform (TREARA, PDSA polymer, 116 nm) with anti-Trop2 antibody and siMNX1-AS1	Active targeting (anti-Trop2) + Relieving Inhibition (GSH scavenging) + Coordinated Regulation	siRNA siMNX1-AS1
2022 [120]	X-ray (12 Gy)	↑ radiosensitization, ↑ antigen capture, ↑ TLR-9 activation, ↑ IFN-β, ↑ M1/M2 ratio, ↑ DC activation, ↑ $CD8^+$ T cell infiltration, ↓ Tregs, ↑ *in situ* vaccine effect, synergizes with anti-CTLA-4, induces abscopal effect and immune memory	PIC: Poly-L-lysine (PLL) + iron oxide nanoparticle (ION) + CpG ODN (hydrodynamic ~110 nm, positive charge)	Active Activation (CpG as TLR-9 agonist) + Coordinated Regulation (radiosensitization, antigen capture, M2→M1 repolarization) + Multimodal (RT + ICB + nanoparticle)	DNA CpG ODN 1826 (sequence NR)

Note: ↑ and ↓ indicate an increase/upregulation and a decrease/downregulation, respectively.

3. Precise Delivery: Passive Targeting, Active Targeting, and Spatiotemporal Activation

3.1. Passive Targeting: A Foundational Concept with Inherent Limitations

The enhanced permeability and retention (EPR) effect provided the original rationale for many oncologic nanoparticles. For nucleic acids, passive accumulation remains useful because prolonged circulation and nanoscale size can increase tumor exposure relative to free oligonucleotides [18,27]. Many of the current systems still rely on this baseline principle. Yet for radiosensitization, passive targeting alone is usually insufficient [137]. Delivery must cope with heterogeneity in tumor vascular permeability, interstitial pressure, stromal density, macrophage sequestration, and, in brain tumors, the BBB/BBTB [138]. Moreover, a radiosensitizer should ideally accumulate where radiation is delivered and release its cargo when the biological need is greatest, rather than only where leaky vasculature happens to exist [139,140].

This limitation is evident in glioblastoma, where systemic delivery of naked siRNA is ineffective because of poor BBB permeability and rapid clearance [36]. Similar constraints apply to metastatic or distant lesions, which may not share the vascular features of the irradiated primary tumor. Passive targeting, therefore, remains a layer of the solution, not the solution itself.

3.2. Active Targeting Improves Anatomical and Cellular Precision

Active targeting can be implemented at several levels: tissue entry, tumor cell binding, immune cell engagement, or subcellular localization. The A1 corpus provides several strong examples.

Tang et al. developed a selenium-engineered mesoporous silica nanocapsule that carries siCFL1 and is decorated with angiopep-2, exploiting LRP1-mediated BBB transcytosis and glioblastoma targeting [36]. As shown in Figure 2a, this platform illustrates two important points. First, active targeting can be indispensable when the therapeutic site is anatomically protected. Second, targeting is most useful when paired with conditional release, because mere entry into tumor cells does not guarantee cytosolic siRNA action. In Tang's study, irradiation-triggered ROS cleaved the diselenide-bridged silica framework, causing matrix collapse and burst release of siCFL1 within irradiated radioresistant glioblastoma, leading to efficient CFL1 knockdown and reduced invasion [36].

Aptamer-directed targeting is another powerful strategy. Chen et al. used a PD-L1 aptamer to guide gold-MnO_2 nanoflowers to tumor cells while simultaneously contributing checkpoint-targeted activity [39]. Ren et al. extended this logic by using PD-L1-targeting aptamers on fusogenic liposomes, allowing melanoma-selective membrane fusion and surface anchoring of programmable aptamer assemblies [38]. The design of this multivariate-gated system is illustrated in Figure 2b. The liposome circulates stably, binds to PD-L1-positive melanoma cells, fuses with the tumor membrane, and anchors aptamer assemblies on the cell surface. Only after radiation-induced ATP release and MMP-2 upregulation does it release the CpG-like immune adjuvant through an AND-gate mechanism. The targeting specificity of the aptamer components was confirmed by flow cytometry. As shown in Figure 2c, the PD-L1 aptamer (aptPD-L1) exhibited 410% higher binding to B16F10 melanoma cells compared to splenocytes, consistent with the elevated PD-L1 expression on cancer cells. In contrast, the engineered CpG (eCpG) showed preferential binding to dendritic cells (220% over other populations), indicating that the two aptamer motifs are orthogonally directed toward their intended cellular targets. This dual-recognition feature ensures that the fusogenic liposomes selectively bind to melanoma cells while the released adjuvant is received primarily by antigen-presenting cells in the tumor microenvironment. The advantage of aptamers over conventional antibodies in these contexts lies not only in size and synthesis, but also in chemical programmability. Aptamers can be integrated with logic-gated architectures that respond to ATP, proteases, or other post-irradiation signals.

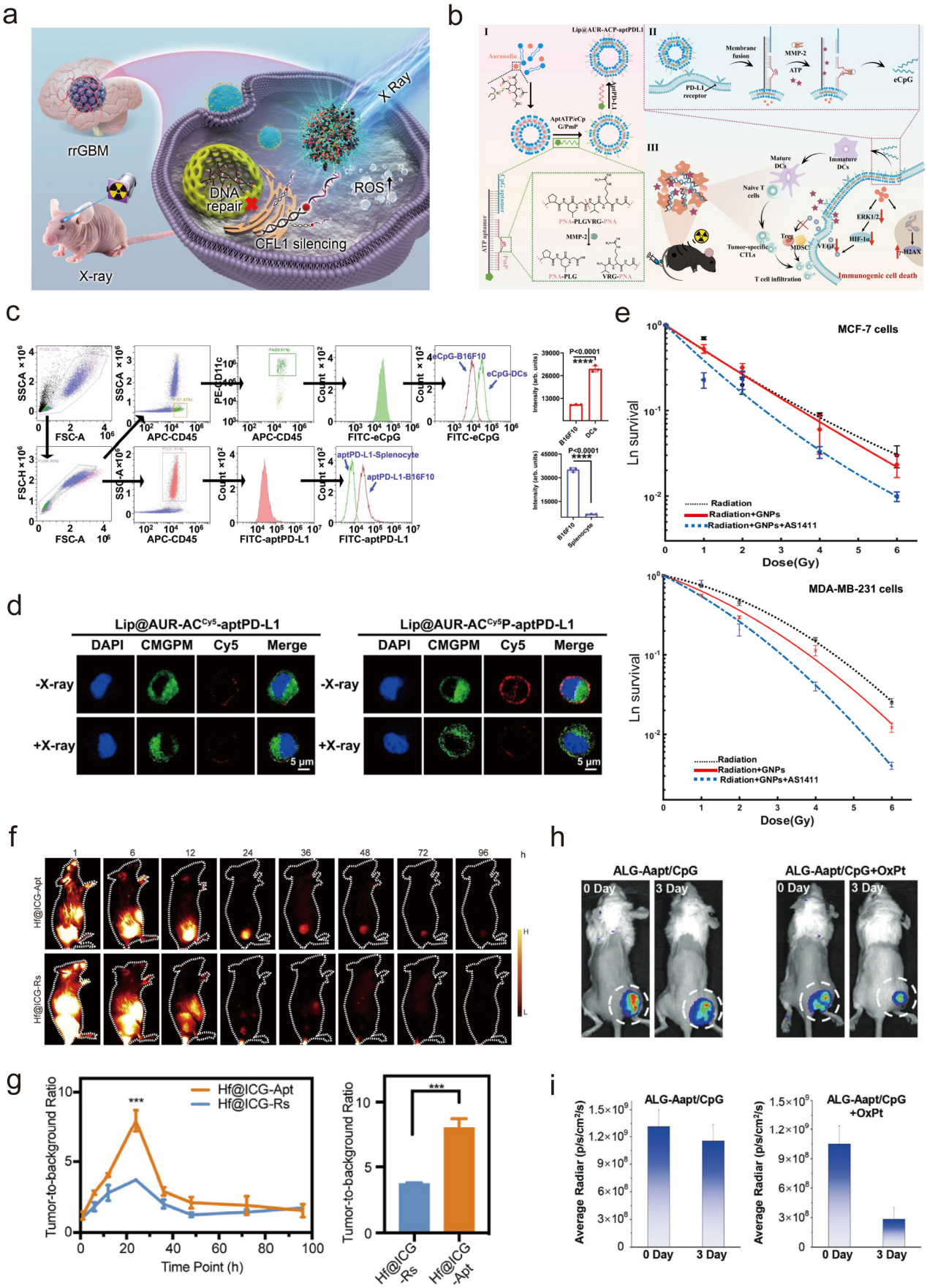

Figure 2. Hierarchical precision delivery strategies for nucleic acid nanomedicines in radiotherapy: (**a**) Schematic illustration of the radiation-triggered selenium-engineered mesoporous silica nanocapsule for siCFL1 delivery in radioresistant glioblastoma. The platform utilizes angiopep-2 for LRP1-mediated blood–brain barrier transcytosis and irradiation-induced ROS to cleave

diselenide bonds for burst siRNA release (Reproduced with permission from Ref. [36] Copyright 2023, American Chemical Society); (**b**) Design of programmable melanoma-targeted fusogenic liposomes functionalized with multivariate-gated aptamer assemblies (ACP) and PD-L1 aptamers. The system employs an AND-gate logic operation requiring both ATP and MMP-2—signals upregulated by radiotherapy—to trigger eCpG release and (**c**) Flow cytometry showing the preferential binding of aptPD-L1 to B16F10 melanoma cells (410% higher than splenocytes) and eCpG to DCs (220% higher than other cells), confirming the cell-type specificity of the targeting components,statistical analysis was carried out via one-way ANOVA method, **** indicates significance at $p < 0.0001$ and (**d**) CLSM images of eCpG release *in vivo*: without IR, eCpG (Cy5, red) is retained on B16F10 membranes; after 4 Gy IR, the signal is almost completely released, validating the AND-gate operation in the tumor microenvironment (Reproduced with permission from Ref. [38] Copyright 2024, Ren et al.); (**e**) Clonogenic survival curves of breast cancer cells treated with AS1411 aptamer-conjugated gold nanoparticles (AS1411/GNPs) under 4 MeV electron beam irradiation. Sensitizer enhancement ratios (SER) were 1.35, 1.66, and 1.91 for MCF-7, MDA-MB-231, and mammosphere cells, respectively (Reproduced with permission from Ref. [126] Copyright 2021, Mehrnia et al.); (**f**) NIR-II fluorescence imaging and (**g**) TBR analysis of 4T1-PD-L1 tumor-bearing mice injected with Hf@ICG-Apt and Hf@ICG-Rs at various time points and after 24 h, the statistical difference is marked with *** (Reproduced with permission from Ref. [133] Copyright 2023, Wei et al.); (**h**) Representative images and (**i**) quantitative analysis show that CpG-Cy5 fluorescence was largely retained in tumors without OxPt treatment, but was markedly diminished following OxPt-triggered ATP release, demonstrating synchronized immune adjuvant release in response to an ICD-inducing therapy. (Reproduced with permission from Ref. [118] Copyright 2021, John Wiley and Sons). In the schematic panels, arrows indicate the direction of material assembly, cellular transport, stimulus-responsive release, or downstream biological effects, as labeled; irradiation symbols indicate X-ray exposure; and mouse schematics denote the corresponding *in vivo* tumor models. In panel (**d**), blue, green, and red fluorescence denote DAPI, CMGPM-stained cell membranes, and Cy5, respectively. In panel (**e**), black dotted, red solid, and blue dashed curves represent radiation alone, radiation + GNPs, and radiation + GNPs + AS1411, respectively. In panel (**g**), orange and blue curves represent Hf@ICG-Apt and Hf@ICG-Rs, respectively.

Zhang et al. proposed a related yet conceptually distinct strategy for metastatic breast cancer. They used T-cell membrane fusion liposomes expressing high levels of PD-1 to target PD-L1-upregulated distant tumors after local RT [40]. This is notable because the targeting ligand exploited not a constitutive tumor marker but a radiotherapy-induced biological state. In other words, RT itself generated the targetable phenotype in the non-irradiated lesion.

The evolution of aptamer-based targeting illustrates a clear progression from generic "homing devices" to functionally integrated modules. Early work using the AS1411 aptamer—which binds to nucleolin overexpressed on many cancer cells—demonstrated that conjugation to 10 nm gold nanoparticles (GNPs) could increase cellular uptake by up to 4-fold in breast cancer cells, leading to a sensitizer enhancement ratio (SER) of 1.35–1.66 under 4 MeV electron beam radiotherapy [126]. Clonogenic survival assays (Figure 2e) demonstrated that AS1411-GNPs at 12.5 mg/L yielded SER values of 1.35 in MCF-7 cells, 1.66 in MDA-MB-231 cells, and 1.91 in mammosphere-derived cancer stem-like cells under 4 MeV electron beam irradiation. The higher SER in the mammosphere suggests that aptamer-mediated targeting can partially overcome the intrinsic radioresistance of stem cell populations. Notably, this SER further increased to 1.91 in mammosphere-derived cancer stem-like cells, suggesting that aptamer-mediated targeting can partially overcome the intrinsic radioresistance of stem cell populations. However, a limitation of AS1411 is its lack of tumor-subtype specificity.

A more refined approach emerged with the GMT8 aptamer, which selectively binds to U87 glioma cells. Li and colleagues functionalized PEGylated Ag@Au core–shell nanoparticles with the GMT8 aptamer, which selectively binds to U87 glioma cells [122]. The GMT8-conjugated nanoparticles achieved a sensitizer enhancement ratio (SER) of 1.62, whereas non-targeted controls yielded an SER of 1.31, and median survival in an orthotopic glioma model was prolonged from 45.5 to 58.5 days. The field has since moved toward functionally integrated aptamers that combine targeting with immune checkpoint blockade and imaging. Wei and colleagues anchored a PD-L1 aptamer onto mesoporous hafnium oxide nanoparticles (Hf@ICG-Apt) [133]. The Hf core acted as a high-Z radiosensitizer, while the aptamer shell enabled tumor-specific delivery and simultaneous PD-L1 blockade. Importantly, the nanoparticles degraded at low pH in

the tumor microenvironment, releasing the near-infrared dye ICG for NIR-II imaging, achieving a tumor-to-background ratio of 7.97 ± 0.76 with sustained retention beyond 48 h (Figure 2f,g). Together, these three studies illustrate a trajectory: from a generic aptamer (AS1411) to a tumor-specific one (GMT8) and finally to a multifunctional aptamer platform that simultaneously delivers a radiosensitizer, a checkpoint inhibitor, and an imaging probe—a shift from "passive accumulation plus a targeting ligand" toward "the aptamer as a therapeutic module".

3.3. Delivery Precision Is Hierarchical, Not Binary

The common discussion of "passive versus active" targeting is often too simplistic. In practice, successful platforms operate through a hierarchy of precision:

1. Circulation-level precision, achieved through size control, PEGylation, membrane camouflage, or extracellular vesicle biology.
2. Tissue-level precision, through EPR, barrier-crossing ligands, or biodistribution bias.
3. Cell-level precision, via receptor ligands such as PD-L1 aptamers, angiopep-2, or membrane proteins.
4. Subcellular precision, through endosomal escape, membrane fusion, or nuclear delivery.
5. Temporal precision, through triggers such as ROS, ATP, MMP-2, hypoxia, or irradiation itself.

This hierarchy is especially clear in Ren et al.'s liposomal system. The liposome circulates stably, binds to PD-L1-positive melanoma cells, fuses with the tumor membrane, and anchors aptamer assemblies on the cell surface. Only after radiation-induced ATP release and MMP-2 upregulation does it release the CpG-like immune adjuvant through an AND-gate mechanism [38]. Similarly, Tang et al.'s nanocapsules cross the BBB, accumulate in radioresistant glioblastoma, escape lysosomes, and release siRNA only when ROS is boosted by irradiation [36]. These examples suggest that delivery precision should be viewed less as "where the nanoparticle goes" than as the number of biological checkpoints it can satisfy before activation.

3.4. Barrier-Penetrating and Membrane-Fusion Systems

For central nervous system disease, barrier penetration remains paramount. Liu et al. used Ang/TAT dual-modified extracellular vesicles to deliver Cas9 protein/sgRNA complexes across the BBB and into glioblastoma tissue, achieving high *in vivo* editing efficiency against GSS with minimal off-target editing [23]. Compared with synthetic nanoparticles, EV-based systems may offer reduced immunogenicity, biological membrane compatibility, and endogenous trafficking properties. Their drawback lies in manufacturing standardization and cargo loading reproducibility, both of which remain significant translational barriers.

Membrane-fusogenic systems represent another notable trend. Rather than relying solely on endocytosis, these platforms can directly merge with tumor membranes, improving cytosolic delivery and surface programming. In Ren et al., fusogenic liposomes enhanced targeted AUR delivery and retained aptamer assemblies on the melanoma cell surface, thereby enabling post-irradiation logic-gated release [38]. This is mechanistically elegant because it separates the functions of entry and activation.

3.5. Radiation as a Delivery Gate

One of the most important advances in the field is the reframing of RT as a delivery gate. Irradiation can increase ROS, induce ATP release, upregulate MMP-2, exacerbate local hypoxia, and alter checkpoint expression. When nanoparticles are designed to read these signals, RT becomes part of the carrier design rather than merely the co-treatment.

Radiotherapy not only kills tumor cells but also creates transient biochemical and cellular conditions that can be exploited as gates for triggered drug release. Three paradigms are particularly relevant. First, radiation-induced metabolites can act as triggers: in the ALG-Aapt/CpG hydrogel, ATP released by dying

cells competitively displaced CpG, synchronizing adjuvant release with antigen availability (Figure 2h) [118]. Second, radiation-associated hypoxia or redox stress can switch responsive polymers from stable to cargo-releasing states, as shown by a metronidazole-containing RNAi nanomedicine that released paclitaxel and siPGK1 in hypoxic glioblastoma [127]. Third, AND-gate designs can require more than one post-RT cue. In Ren et al.'s fusogenic liposome, as shown in Figure 2d, eCpG release required both ATP and MMP-2, restricting immune activation to irradiated PD-L1-positive tumors [38]. Timing is also part of the gate: spherical nucleic acids delivered at the macrophage-recruitment peak after low-dose RT achieved markedly deeper tumor penetration [124]. Together, these examples support a central design principle: the radiation beam defines where and when the nanomedicine becomes active.

This principle may be more clinically relevant than maximizing passive accumulation alone. Tumors are heterogeneous at baseline, but irradiation creates a spatiotemporally defined microenvironment in the treatment field. A carrier that responds to that field is, in effect, aligned to the treatment plan.

4. Target Selection: Single Attack or Coordinated Regulation?

4.1. The Appeal of the Single Dominant Target

A dominant-node strategy has clear strengths. It simplifies biomarker development, facilitates mechanistic interpretation, and reduces formulation complexity. Tang et al. targeted CFL1, a driver of actin remodeling, migration, and radioresistant infiltration in glioblastoma [36]. Wang et al. targeted circADARB1, showing that it promoted nasopharyngeal carcinoma radioresistance through the miR-615-5p/HSP90B1/SLC7A11-GPX4 axis and suppression of ferroptosis [136]. The design of their biomimetic nanocarrier (Fe@Pdots-siRNA) is illustrated in Figure 3a. This platform co-delivers si-circADARB1 and iron ions, simultaneously silencing the circular RNA that stabilizes the SLC7A11/GPX4 ferroptosis defense machinery while providing the catalytic iron required for lipid peroxidation. Liu et al. targeted GSS, a glutathione-synthesizing enzyme identified by *in vivo* CRISPR screening as a mediator of glioblastoma radioresistance [23]. As shown in Figure 3b, they employed Ang/TAT dual-modified extracellular vesicles to deliver Cas9 protein/sgRNA complexes across the BBB and into glioblastoma tissue. GSS depletion disrupted glutathione synthesis, inactivated GPX4, increased iron accumulation, and amplified radiation-induced ferroptosis. In each case, the authors built a compelling biological chain from target dysregulation to radiation response and therapeutic reversal. This strategy is attractive when a target sits near the top of a functionally important module. GSS depletion, for example, disrupted glutathione synthesis, inactivated GPX4, increased iron accumulation, and amplified radiation-induced ferroptosis. Zetrini and colleagues developed polymer-lipid hybrid nanoparticles delivering RAD50 siRNA to triple-negative breast cancer cells [81]. As shown in Figure 3c, RAD50-siRNA-NPs combined with radiotherapy achieved a 2.5-fold increase in tumor growth inhibition and a 4.5-fold increase in apoptosis compared with radiotherapy alone. Quantification of γ-H2AX foci (Figure 3d) revealed that RAD50 silencing resulted in approximately twofold higher initial DNA double-strand breaks, confirming that disruption of the MRN complex component impairs both homologous recombination and non-homologous end joining. In another case, Yu and colleagues developed a coordination-driven FBXW7 DNAzyme-Fe^{2+} nanoassembly coated with hyaluronic acid for CD44-mediated targeting [48]. This system not only stabilized phosphorylated p53 to enforce irreversible G2 arrest but also suppressed the SLC7A11/GSH/GPX4 anti-ferroptosis axis. The dual mechanism increased apoptosis from 8% to 57% *in vitro* and extended median survival from 35 to 59 days in tumor-bearing mice.

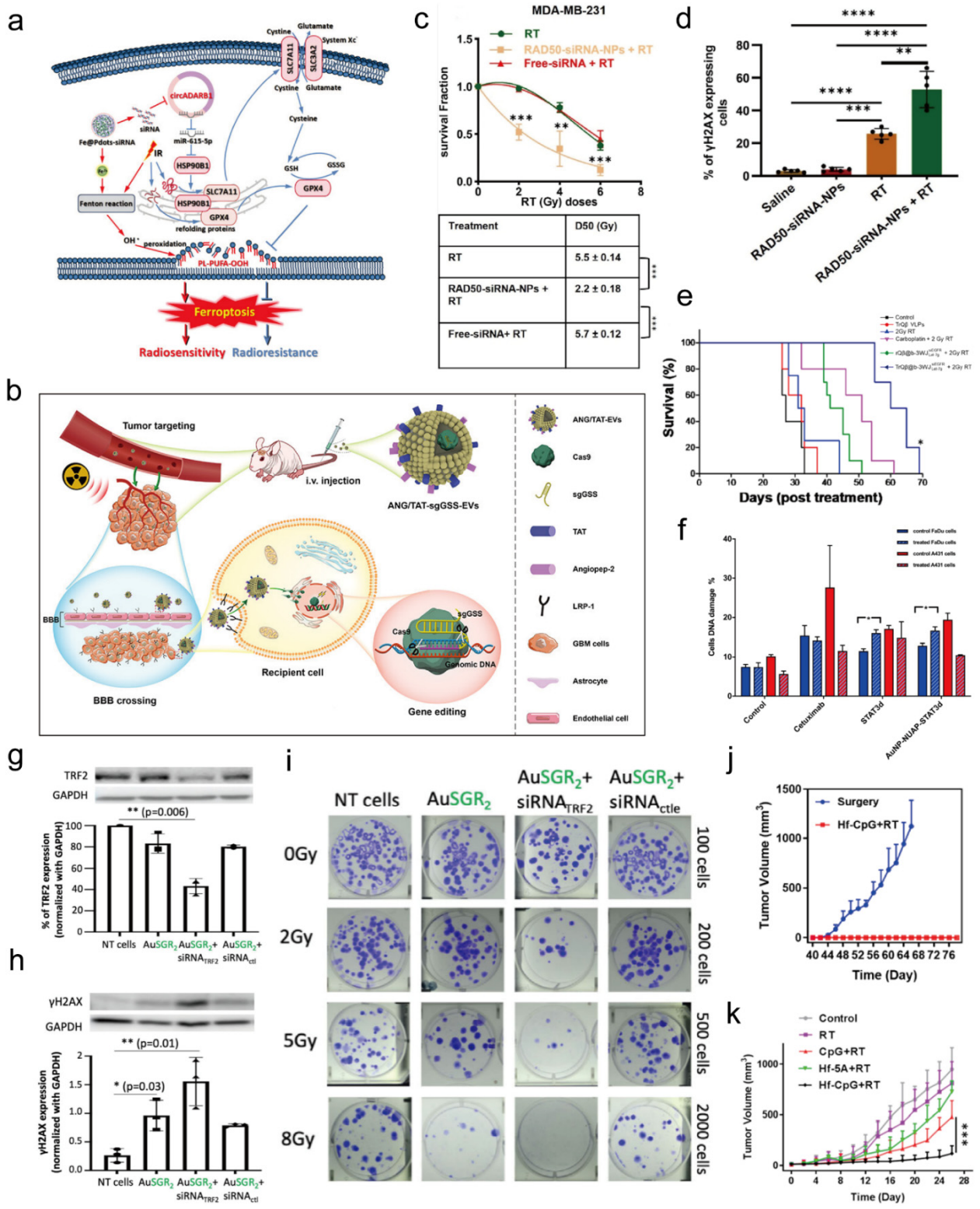

Figure 3. Target architecture in nucleic acid–enabled radiosensitization: from dominant-node silencing to coordinated network regulation. (**a**) Schematic of the biomimetic Fe@Pdots-siRNA nanocarrier for co-delivery of si-circADARB1 and iron ions. In the schematic panels, arrows indicate the direction of molecular transport, signaling, gene editing, ferroptotic responses, or the treatment workflow, as labeled; irradiation symbols indicate radiotherapy; and mouse/tumor schematics denote the corresponding *in vivo* glioblastoma models. This platform promotes ferroptosis and overcomes nasopharyngeal carcinoma radioresistance by targeting the miR-615-5p/HSP90B1/SLC7A11-GPX4 axis (Reproduced with permission from Ref. [136] Copyright 2024, American Chemical Society); (**b**) Schematic of engineered extracellular vesicles (EVs) modified with Angiopep-2 and TAT peptides for CRISPR/Cas9 delivery. The system achieves targeted disruption of GSS to induce ferroptosis and sensitize glioblastoma to radiotherapy (Reproduced with permission from Ref. [23] Copyright 2023, Liu et al.); (**c**) Tumor

growth inhibition in a triple-negative breast cancer model treated with RAD50-siRNA-loaded polymer-lipid hybrid nanoparticles (RAD50-siRNA-NPs) plus radiotherapy, showing a 2.5-fold increase in tumor growth delay compared to radiotherapy alone. $p < 0.05$ was considered statistically significant. ** $p < 0.005$ and *** $p < 0.0005$. (Reproduced with permission from Ref. [81] Copyright 2024, Zetrini et al., published by Elsevier Ltd.); (**d**) Quantification of γ-H2AX foci in TNBC cells pretreated with RAD50-siRNA-NPs, demonstrating an approximately twofold increase in initial DNA double-strand breaks following irradiation, Data are presented as mean ± SD. ** $p < 0.005$, *** $p < 0.0005$, and **** $p < 0.0001$. (Reproduced with permission from Ref. [81] Copyright 2024, Zetrini et al., published by Elsevier Ltd.); (**e**) Survival curves of mice bearing orthotopic glioblastoma treated with bacteriophage Qβ particles carrying a three-way junction RNA scaffold (siEGFR and miRNA Let-7g) plus radiotherapy. Coordinated dual knockdown prolonged median survival from 31 days to over 60 days, * indicates a significant difference (log-rank test, * $p < 0.05$) of TrQβ@b-3WJ $^{siEGFR}_{Let\text{-}7g}$ (5 μM) + 2 Gy X-ray irradiation to all other treatment groups. (Reproduced with permission from Ref. [123] Copyright 2023, Pang et al., published by American Chemical Society); (**f**) γ-H2AX expression in FaDu head and neck cancer cells 24 h after 4 Gy irradiation. Treatment with AuNP-NUAP-STAT3d increased DNA damage by nearly 50%, outperforming the therapeutic antibody cetuximab. * $p < 0.005$ indicates statistical significance. (Reproduced with permission from Ref. [132] Copyright 2018, Zhang et al.); (**g**) Western blot confirming approximately 50% downregulation of TRF2 protein after AuSGR2-siRNATRF2 treatment, both before and after irradiation, and (**h**) γ-H2AX protein levels assessed 96 h post-irradiation, showing substantially elevated DNA double-strand breaks in cells treated with AuSGR2-siRNATRF2 + RT compared to controls , and (**i**) Clonogenic survival assay of A549 lung cancer cells treated with self-assembled AuSGR2-siRNATRF2 nanoclusters plus irradiation (0–8 Gy). The combination reduced the surviving fraction dramatically, yielding a sensitizer enhancement ratio (SER) of 2.3 at 5 Gy This single-target intervention disrupts telomere integrity, impairs DNA repair, and amplifies radiation-induced cytotoxicity (Reproduced with permission from Ref. [135] Copyright 2025, Moro et al.); (**j**) Distant (non-irradiated) tumor growth curves in a bilateral CT26 tumor model, demonstrating that a single intratumoral injection of Hf-CpG MXF plus 8 Gy focal X-ray irradiation completely suppresses the growth of untreated distant tumors—a robust abscopal effect achieved without the need for additional immune checkpoint inhibitors and (**k**) long-term immune memory validation: mice cured by Hf-CpG + RT remained tumor-free upon rechallenge with the same tumor cells, whereas age-matched naïve controls developed tumors rapidly, confirming the establishment of durable protective immunity. This strategy exemplifies coordinated regulation in its most streamlined form: a single coordination entity simultaneously provides high-Z radiosensitization and TLR9-mediated immune activation. The statistical difference is marked with *** (Adapted with permission from Ref. [128] Copyright 2022, American Chemical Society).

In another illustrative case, Moro and colleagues designed self-assembled peptide-gold nanoclusters ($AuSGR_2$) to deliver siRNA targeting TRF2, a shelterin component that protects telomere ends from being recognized as DNA damage [135]. As shown in Figure 3g–i, this single-target intervention triggered profound telomere deprotection and unleashed a cascade of DNA damage responses upon irradiation, resulting in a sensitizer enhancement ratio (SER) of 2.3, approximately 50% knockdown of TRF2 protein, and markedly elevated γ-H2AX levels indicative of unrepaired double-strand breaks. Notably, this degree of radiosensitization was achieved without multi-drug loading, illustrating that a well-chosen dominant node—TRF2, which governs telomere integrity and DNA repair signaling—can simultaneously collapse multiple resistance modules. The platform also featured a straightforward assembly strategy using an arginine-rich peptide to complex siRNA-TRF2 with gold nanoclusters, highlighting that therapeutic potency can be achieved through precise biological targeting rather than formulation complexity.

That is nominally a single-gene intervention, but functionally it collapses an entire antioxidant defense axis.

4.2. The Limits of Monofocal Intervention

The problem is that radioresistance is rarely maintained by a solitary pathway. Hypoxia, metabolic plasticity, immune suppression, DNA repair, and invasive escape can compensate for one another [141]. A tumor that loses one defense may strengthen another. This is why many "single attack" strategies work well preclinically yet struggle to define a path toward broader clinical relevance [142,143].

Even within the papers that appear single-targeted, broader mechanisms are usually at play. CFL1 knockdown reduces invasion, but Tang's platform also incorporates metronidazole-derived components that stabilize radiation-induced DNA lesions under hypoxia [36]. circADARB1 silencing reduces ferroptosis resistance, but Wang's platform simultaneously supplies Fe^{2+} to intensify lipid peroxidation

chemistry [136]. GSS editing amplifies ferroptosis, but the delivery system itself solves BBB penetration and tissue specificity [23]. Thus, the real strategic distinction may not be single versus multiple targets in a superficial counting sense. It may be whether the intervention addresses one isolated molecule or one organizing node plus the compensatory context around it.

4.3. Coordinated Regulation Better Matches Tumor Systems Biology

Coordinated regulation means designing the payload-platform pair to manipulate several interdependent resistance circuits. Ren et al. provide the strongest illustration [38]. Their system does not merely sensitize melanoma cells to radiation via AUR-mediated gold dose deposition. The debate between single-node silencing and coordinated regulation is not merely academic; it directly affects therapeutic outcomes in challenging models. Single-target approaches can be powerful when the target sits atop a critical signaling hub. For instance, silencing PGK1 alone—a key metabolic kinase—enhanced chemo-radiotherapy sensitivity in glioblastoma by depleting ATP and radiosensitizing hypoxic cells [127]. Similarly, targeting TRF2, a telomere-protective protein, with self-assembled peptide-gold nanoclusters increased radiosensitivity 2.3-fold in lung cancer cells [135]. However, when tumors are highly heterogeneous or resistant to single interventions, coordinated regulation becomes essential. A prime example is the simultaneous silencing of EGFR and IKKα via a bacteriophage Qβ particle packaging a three-way junction RNA scaffold carrying both siRNA and miRNA [123]. As shown in Figure 3e, this dual knockdown inactivated NF-κB signaling and suppressed DNA repair. In an orthotopic glioblastoma model, the combination with radiotherapy prolonged median survival from 31 days (radiotherapy alone) to over 60 days, demonstrating the power of coordinated network regulation. Another coordinated strategy used a single nanoplatform to both deplete glutathione (via a poly(disulfide amide) shell) and silence lncMNX1-AS1 (via siRNA), thereby inhibiting JAK3/STAT3 signaling and overcoming radioresistance in triple-negative breast cancer [51]. The sensitization enhancement ratio (SER) of this dual-action system was 1.69, compared with 1.42 for GSH depletion alone, illustrating the advantage of coordinated regulation over single-mechanism intervention. An elegant example of coordinated regulation in a minimalist form was reported by Yang and colleagues, who constructed an Hf-CpG metal–"X" framework (MXF) through direct coordination of Hf^{4+} ions with CpG oligonucleotides [128]. This carrier-free single entity simultaneously performs two functions: the high-Z hafnium component enhances local radiation dose deposition, while the CpG serves as a TLR9 agonist to trigger dendritic cell maturation and downstream T-cell activation. Unlike most combination strategies that require separate delivery vehicles and multiple therapeutic moieties, this MXF represents a genuine convergence of radiosensitization and immune stimulation at the molecular level. A single intratumoral injection of Hf-CpG MXF followed by 8 Gy localized X-ray irradiation not only eradicated primary CT26 tumors in all treated mice but also induced a potent abscopal effect that completely suppressed the growth of untreated distant tumors, without the addition of any immune checkpoint inhibitor (Figure 3j,k). Rechallenged cured mice remained tumor-free, confirming durable immune memory. This study blurs the traditional boundary between "target" and "vehicle", demonstrating that coordinated regulation need not require multicomponent complexity. When the metal-nucleic acid coordination chemistry inherently addresses both the physical and immunological barriers to tumor control, a single well-designed platform can achieve what normally demands multimodal integration. These examples argue that the optimal target architecture is context-dependent: a dominant node suffices for some tumors, but a network-level intervention is necessary for those with built-in redundancy. It also suppresses ERK1/2-HIF-1α-VEGF signaling, limiting recruitment of immunosuppressive cells; exploits RT-induced ATP and MMP-2 as logic inputs; and releases CpG-like adjuvant to promote dendritic-cell maturation and adaptive immunity. Here, the relevant target is not a single gene but a radio-immunological program.

Chen et al. similarly combined high-Z-mediated radiation enhancement, MnO_2-mediated hypoxia relief, PD-L1 targeting, BMS-202 checkpoint inhibition, macrophage reprogramming, and photothermal

augmentation of ICD [39]. Zhang et al. combined an iodine-containing cyanine radiosensitizer, CpG immune activation, PD-1/PD-L1-mediated distal targeting, and direct modulation of MDSC function in distant tumors [40]. These studies suggest that the most robust systems are those in which multiple mechanisms are not simply added together but linked through a coherent biological rationale.

Two contrasting but equally instructive strategies have further sharpened the debate between single-node silencing and coordinated regulation. On one hand, as previously described, a minimalist, carrier-free approach was reported by Yang and colleagues, who constructed an Hf-CpG metal-"X" framework (MXF) through direct coordination of Hf^{4+} ions with CpG oligonucleotides [128]. This single entity achieves two functions at once: the high-Z Hf enhances local radiation dose deposition, and the CpG acts as a TLR9 agonist to trigger dendritic cell maturation. Unlike most combination strategies, this MXF does not require additional immune checkpoint inhibitors. A single intratumoral injection of Hf-CpG followed by 8 Gy X-ray irradiation completely eradicated primary CT26 tumors in all mice, induced a strong abscopal effect on distant tumors, and provided long-term immune memory (rechallenged mice remained tumor-free 40 days after primary tumor excision). This platform represents a third paradigm between single-agent radiosensitization and multi-component nanocarriers: it leverages coordination chemistry to create a self-adjuvanting radiosensitizer, blurring the boundary between "target" and "vehicle".

On the other hand, a conceptually distinct single-node intervention was demonstrated by Zhang and colleagues, who engineered a gold nanoparticle carrying a nucleolin aptamer (NUAP) for tumor targeting and a STAT3 decoy (STAT3d) that sequesters activated STAT3 [132]. As shown in Figure 3f, this dual construct increased DNA damage (γ-H2AX) by nearly 50% after 4 Gy irradiation in FaDu head and neck cancer cells, outperforming the standard therapeutic antibody cetuximab. Remarkably, this sensitization was achieved with only 88 nM STAT3d—a five-fold lower concentration than free STAT3d—demonstrating that the AuNP not only protects the oligonucleotide but also enhances its nuclear delivery. This mechanism is distinct from checkpoint blockade: rather than releasing the brake on already-primed T cells, STAT3 inhibition directly reduces tumor cell survival signaling and promotes apoptosis. Thus, the optimal target architecture is context-dependent: the MXF exemplifies coordinated regulation (radiosensitization plus immune adjuvant) that achieves systemic immunity without ICB, while the STAT3 decoy shows that a well-chosen single node can be remarkably effective when delivered with precision. Both strategies challenge the assumption that "more targets are always better"—what matters is whether the intervention matches the specific resistance circuitry of the tumor.

4.4. A Practical Framework for Target Architecture

For radiosensitizer design, target architecture can be grouped into three operational categories.

1. Dominant-node silencing;

Examples include CFL1, circADARB1, or GSS [23,36,136]. This is most useful when a single target governs a major bottleneck, and the tumor type is biologically well characterized.

2. Dominant-node silencing plus contextual amplifier;

Examples include a single nucleic acid target paired with Fe-mediated ferroptosis chemistry, metronidazole-based hypoxia fixation, or photothermal ICD enhancement [36,39,136]. This is likely more clinically resilient than Type I because it anticipates compensatory biology.

3. Coordinated network regulation;

Examples include simultaneous radiosensitization, checkpoint control, myeloid suppression, and immune adjuvant release [38–40]. These are conceptually closest to the systems biology of real tumors, but they pose the greatest manufacturing and regulatory complexity.

The field is increasingly moving from Type I toward Type II and Type III. That trend appears justified. Radiosensitization should not be thought of as a single biochemical event. It is a change in the balance between damage, repair, escape, and immunity.

5. Immune Remodeling: From Relieving Inhibition to Active Activation

5.1. Irradiation Is Immunogenic, but Incompletely So

RT can induce ICD and release DAMPs such as ATP, HMGB1, and calreticulin, thereby facilitating antigen presentation and T-cell priming [6,12,39]. It can also promote chemokine release and, in some settings, abscopal effects. Yet irradiation alone often produces only a modest immune response. The reasons are now clear: suppressive myeloid populations persist, checkpoint molecules are upregulated, antigen-presenting cells are incompletely activated, and T cells entering the tumor may remain dysfunctional [12–15,39].

This has led to two broad strategies. The first is relieving inhibition—blocking PD-L1, reducing MDSCs, suppressing VEGF-driven myeloid recruitment, or repolarizing M2-like macrophages. The second is active activation—delivering CpG, promoting dendritic-cell maturation, increasing $CD8^+$ T-cell priming, and building immune memory. The conceptual evolution from the first to the second is central to the current field.

5.2. Relieving Inhibitory Constraints

Checkpoint-oriented systems are now common. Chen et al. used a PD-L1 aptamer and BMS-202 to enhance T-cell activation while also increasing ROS generation and ICD [39]. Ren et al. used PD-L1 aptamers not only for targeting but also to help address post-irradiation PD-L1 elevation [38]. Checkpoint blockade remains a cornerstone of radio-immunotherapy, but the molecular target and delivery route profoundly affect efficacy. While PD-L1 aptamers have been widely used to block the PD-1/PD-L1 axis, recent studies reveal that PD-L2 on CAFs can be equally immunosuppressive. A PD-L2-targeted nanoparticle that simultaneously blocks PD-L2 and reprograms CAFs into αPD-L1-secreting factories achieved superior T-cell reactivation compared to systemic anti-PD-L1 antibody [111]. As shown in Figure 4a, this system converts immunosuppressive CAFs into antigen-presenting cells that express CD86 and secrete αPD-L1 antibodies locally, turning a pro-tumor ally into an anti-tumor factory without the structural damage caused by CAF depletion. Meanwhile, siRNA-mediated PD-L1 silencing offers an advantage over antibodies: it also downregulates intracellular PD-L1, which otherwise binds and stabilizes DNA repair mRNAs (BRCA1, MRE11, RAD50). Boron nanoparticles loaded with PD-L1 siRNA not only sensitized tumors to BNCT but also amplified DNA damage and immunogenic cell death [82]. These findings challenge the conventional view that checkpoint inhibition is solely about blocking surface receptors; intracellular pools of checkpoint proteins can also be therapeutically targeted. Zhang et al. exploited RT-induced PD-L1 upregulation in distant tumors to improve distal targeting of PD-1-displaying liposomes and simultaneously downregulate PD-L1 expression there [40]. These studies treat checkpoint biology not just as a barrier to be removed, but as a source of selective information.

Suppression of immunosuppressive myeloid cells is equally important. In Ren et al., AUR inhibited ERK1/2-HIF-1α-VEGF signaling, decreasing MDSC and Treg infiltration [38]. Chen et al. reported reduced M2-like macrophages in tumors treated with their multifunctional nanoradiosensitizer [39]. Zhang et al. found that their CIFL platform directly reduced the number and suppressive activity of MDSCs in distant tumors and metastatic lesions, including decreased ARG1 activity and diminished inhibition of $CD8^+$ T-cell proliferation [40]. These findings are significant because they show that post-RT immune escape is not dominated solely by T-cell checkpoints. The myeloid compartment often determines whether antigen release results in productive immunity or immunological paralysis.

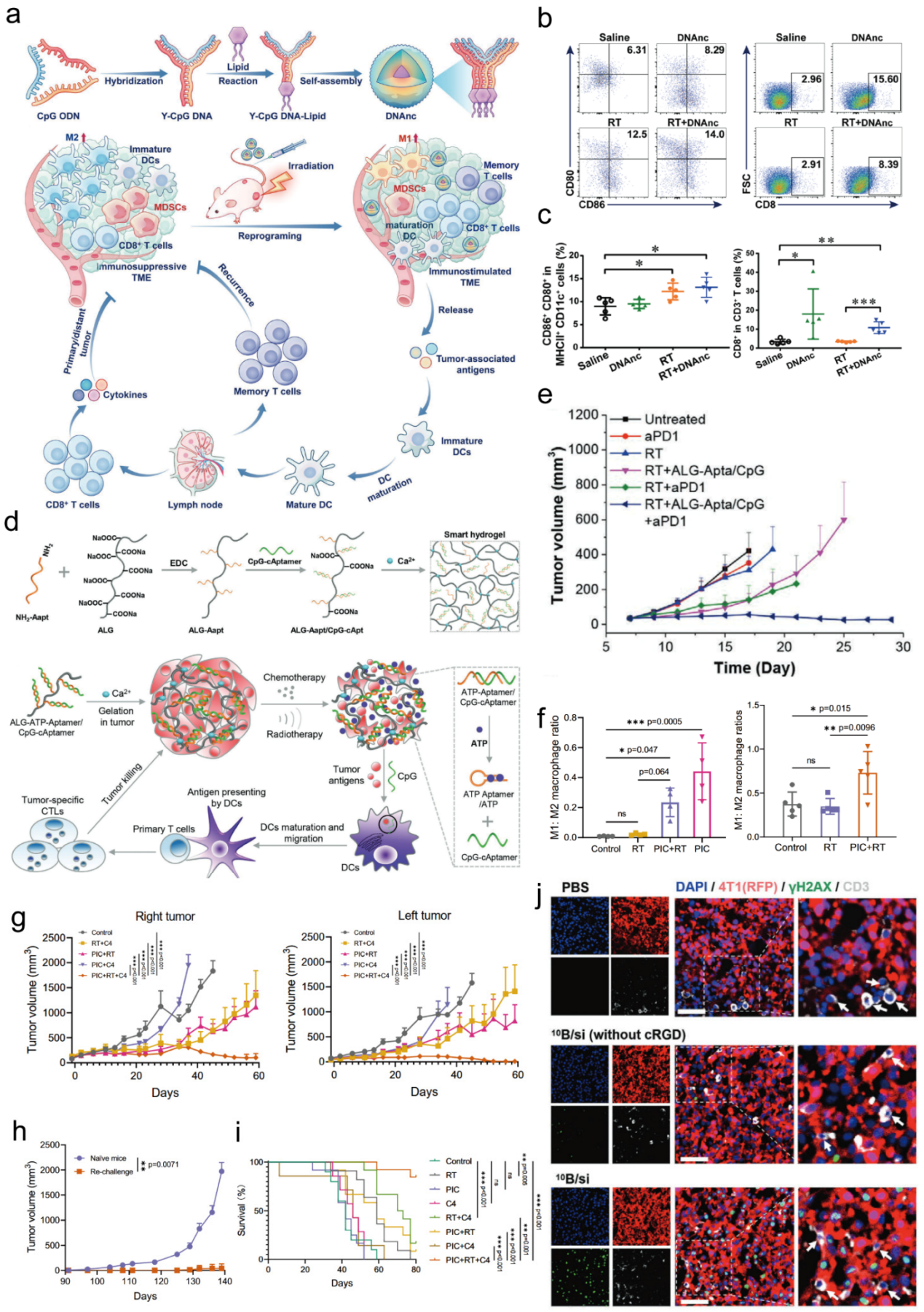

Figure 4. Immune remodeling in radio-immunotherapy: evolution from checkpoint relief to active immune instruction. (**a**) Schematic illustration of the DNA nanocluster (DNAnc) self-assembled from CpG-ODN-loaded Y-shaped DNA vectors, and its

antitumor mechanism via repolarizing M2-like macrophages to M1-like macrophages after radiotherapy and (**b**) representative flow cytometric pseudocolor plot of mature DCs ($CD80^+CD86^+$ in $MHCII^+CD11c^+$) (n = 5) and $CD8^+$ T cells ($CD8^+$ in $CD3^+$) (n = 5) and (**c**) corresponding quantitative analysis modulation by DNAnc. DNAnc carrying ~8125 CpG copies per particle increased the $CD8^+$ T-cell/Treg ratio by sixfold following single-dose radiotherapy, all data are presented as mean ± SD. * p < 0.05, ** p < 0.01, *** p < 0.001 between the indicated groups. (Adapted with permission from Ref. [112] Copyright 2023, John Wiley and Sons); (**d**) Schematic of the ATP-responsive ALG-Aapt/CpG hydrogel: radiotherapy-induced ATP release from dying tumor cells competitively displaces CpG from the hydrogel, synchronizing immune adjuvant delivery with antigen availability and (**e**) Distant tumor growth curves in a bilateral tumor model. Local treatment with ALG-Aapt/CpG hydrogel plus radiotherapy significantly inhibited the growth of untreated distal tumors (Adapted with permission from Ref. [118] Copyright 2021, John Wiley and Sons); (**f**) The ratios of M1:M2 macrophage in $CD11b^+F4/80^+$ BMDMs at day 4 after indicated treatment and quantification of M1/M2 macrophage ratio in tumors treated with PIC nanoparticles. PIC treatment increased the M1/M2 ratio from 0.21 to 0.50, and (**g**) abscopal effect induced by PIC nanoparticles. In a bilateral B78 melanoma model, treatment with PIC + RT + anti-CTLA-4 significantly suppressed the growth of both the directly treated (right flank) and untreated distant (left flank) tumors compared to all other groups, and (**h**) long-term immune memory validation by PIC + RT + anti-CTLA-4 treatment. Mice rendered tumor-free by the triple combination remained tumor-free upon rechallenge with the same B78 melanoma cells, whereas all naïve controls developed tumors, confirming the establishment of durable, tumor-specific immunological memory and (**i**) survival benefit of the triple combination. Kaplan-Meier survival curves of B78 melanoma-bearing mice showing that PIC + RT + anti-CTLA-4 significantly prolonged overall survival compared to all other treatment groups (Adapted with permission from Ref. [120] Copyright 2022, Zhang et al.); (**j**) T cell immunity enhancement by boron neutron capture therapy (BNCT). ^{10}B/siPD-L1 nanoparticles precisely killed tumor cells while sparing adjacent T cells, inducing potent antitumor immunity against distal tumors. White arrows indicate $CD3^+$ T cells, which exhibit minimal γ-H2AX staining compared with adjacent 4T1-RFP tumor cells. (Adapted with permission from Ref. [82] Copyright 2025, John Wiley and Sons). ns = not significant.

5.3. Active Immune Instruction

The more recent conceptual shift is toward active immune instruction. Instead of merely removing brakes, these systems provide a positive signal to the immune system. CpG is a key example. In Ren et al., an engineered CpG aptamer-based immunoadjuvant was released only after radiation-induced ATP and MMP-2 signals triggered an AND-gate mechanism, leading to dendritic-cell maturation and downstream T-cell activation [38]. Sun and colleagues designed an ATP-responsive alginate-based hydrogel (ALG-Aapt/CpG) that synchronizes immune adjuvant release with radiotherapy-induced immunogenic cell death [118]. The design principle is illustrated in Figure 4d. The hydrogel remains inert until radiotherapy triggers ATP release from dying tumor cells; ATP then competitively displaces CpG from the hydrogel, ensuring that the “danger signal” (CpG) is released precisely when tumor antigens are also being shed. In bilateral tumor models, the ALG-Aapt/CpG hydrogel combined with local radiotherapy significantly inhibited the growth of untreated distant tumors and increased the percentage of $CD8^+$ T cells in distal lesions (Figure 4e). This demonstrates that synchronizing immune adjuvant release with antigen availability can generate systemic antitumor immunity from a localized radiation event.

In Zhang et al., CpG co-delivered with the cyanine radiosensitizer enhanced dendritic-cell maturation, promoted inflammatory cytokine release, and improved systemic control of distant lesions after local RT [40]. Moving beyond checkpoint blockade, active immune instruction aims to directly educate antigen-presenting cells. CpG oligonucleotides are potent TLR9 agonists, but their efficacy is limited by rapid degradation and poor cellular uptake. To overcome this, Xie and colleagues developed DNA nanoclusters (DNAnc) that package approximately 8125 CpG copies per particle, rendering them resistant to nuclease degradation and capable of sustaining cytokine release for up to 72 h. The design principle is illustrated in Figure 4a, where Y-shaped DNA vectors loaded with CpG ODNs self-assemble into a clustered nanostructure. As shown in Figure 4b,c, DNAnc combined with single-dose radiotherapy repolarized tumor-associated macrophages from M2 to M1 phenotype and increased the $CD8^+$ T-cell/Treg ratio by six-fold, whereas free CpG lost activity within 24 h [112]. When combined with single-dose radiotherapy, DNAnc repolarized tumor-associated macrophages from M2 to M1 phenotype and increased the $CD8^+$ T-cell/Treg ratio by 6-fold. An orthogonal approach used a multifunctional nanoparticle composed of

polylysine, iron oxide, and CpG (PIC). As shown in Figure 4f, this positively charged particle captured tumor antigens released by radiotherapy and delivered them together with CpG to dendritic cells, increasing the ratio of M1:M2 macrophages from 0.21 to 0.50 and curing 69% of mice when combined with anti-CTLA-4 [120]. Thus, providing both the adjuvant (CpG) and a favorable metabolic environment (oxygen) synergistically amplifies adaptive immunity.

This evolution matters because checkpoint blockade alone cannot compensate for inadequate priming. A T cell cannot be "unleashed" if it was never effectively generated. From this perspective, the immune role of nucleic acid therapeutics in radiosensitization is no longer just to block PD-L1 or reduce suppressive cells, but to convert irradiation into a more complete vaccination event.

5.4. Abscopal and Memory Effects as Benchmarks of Immune Remodeling

The most meaningful evidence that immune remodeling has moved beyond local radiosensitization is the emergence of abscopal and memory outcomes. Chen et al. reported suppression of untreated distant tumors in a bilateral 4T1 model, along with increased dendritic cell maturation, $CD8^+$ T-cell infiltration, and effector-memory T-cell formation [39]. Ren et al. reported systemic control of distal melanoma tumors and expansion of memory $CD8^+$ T cells in bilateral models [38]. Zhang et al. demonstrated reduction of distal tumor growth and suppression of lung metastases, accompanied by increased $CD8^+$ T-cell signals and reduced MDSCs in metastatic lesions [40]. The multifunctional PIC (polylysine–iron oxide–CpG) nanoparticle platform developed by Zhang et al. provides a comprehensive illustration of how active immune instruction translates into systemic and durable antitumor immunity. As shown in Figure 4g, in a bilateral B78 melanoma model, the combination of intratumoral PIC injection, local radiotherapy (12 Gy), and systemic anti-CTLA-4 not only controlled the directly treated primary tumor but also significantly suppressed the growth of the distant, untreated tumor on the contralateral flank, with 4 out of 9 mice achieving complete tumor regression. Crucially, this platform elicited long-term protective immunity. Upon rechallenge with the same B78 melanoma cells 91 days after the initial treatment, 80% of the mice that had been rendered tumor-free by PIC + RT + anti-CTLA-4 rejected the secondary tumor challenge, whereas all naïve controls developed rapidly progressing tumors (Figure 4h). Corresponding splenocyte co-culture assays confirmed the presence of tumor-specific memory T cells. The therapeutic impact of this immune remodeling was reflected in a marked survival advantage: mice receiving the triple combination showed significantly prolonged overall survival compared to RT + anti-CTLA-4 alone or any doublet therapy (Figure 4i) [120]. These results collectively demonstrate that a rationally designed nanoplatform, when timed with radiation, can convert a local treatment into a systemic and durable vaccine-like response.

These findings should not be overinterpreted as direct analogues of human metastatic control, but they are important because they shift the endpoint of radiosensitizer development. The benchmark is no longer only local clonogenic kill. It is whether a platform can reshape the systemic immune consequences of localized irradiation.

5.5. Immunologically Informed Sequencing: Aligning Nano-Immunotherapy with Radiotherapy Dynamics

The growing recognition that the timing of immunotherapy relative to radiotherapy fundamentally shapes therapeutic outcomes, as articulated in the comprehensive review by Darragh and Karam [144], has profound implications for the design of nucleic acid-loaded nanoradiosensitizers. Their analysis emphasizes a critical principle: radiotherapy can prime the immune system by releasing tumor antigens and activating dendritic cells, but if immune checkpoint blockade (ICB) is administered too early, the expanding T cell clones may be inadvertently damaged by subsequent radiation fractions. This insight directly informs how nano-delivery systems should be temporally coordinated with radiation.

Consistent with this framework, several nanomedicine studies have inadvertently validated the principle that delivering immune-modulating nucleic acids after the initial radiation insult may be more effective. In the work by He and colleagues, the metformin-based nanoplatform (CSMT) delivering siTREX1 was administered intravenously, with a 24-h interval before local irradiation [134]. This scheduling allowed the nanocomplex to accumulate in tumors and begin its biological amplification of DNA damage precisely in synchrony with radiation delivery, leading to robust STING pathway activation and systemic antitumor immunity. Similarly, the ATP-responsive hydrogel designed by Sun and colleagues released the immune adjuvant CpG only after radiotherapy triggered ATP release from dying tumor cells, ensuring that immune stimulation occurred during the peak of antigen availability rather than before [118]. This "post-radiation" timing aligns with the principle that immunotherapy should amplify, rather than precede, the antigen presentation cascade initiated by radiotherapy.

Conversely, studies that administered immune-modulating agents before or concurrently with all radiation fractions may have inadvertently attenuated optimal T cell expansion. The work by Deng and colleagues, which delivered PD-L1 siRNA-loaded boron nanoparticles before BNCT, achieved significant radiosensitization [82]. However, from an immunological sequencing perspective, delivering ICB before the full course of radiation could potentially expose expanding T cell clones to subsequent radiation fractions, a concern mitigated in that study using BNCT, which is inherently more tumor-selective and spares circulating lymphocytes. The concept of "spacing" fractions, as highlighted by the Personalized Ultrafractionated Stereotactic Adaptive Radiotherapy (PULSAR) approach, also finds resonance in nanomedicine design. The hypoxia-triggered RNAi nanomedicine developed by Wang and colleagues was administered intravenously, with radiation delivered after a 12-h window to allow for tumor accumulation and payload release [127]. This scheduling, while not explicitly designed to optimize T cell priming intervals, inadvertently allowed for a temporal gap that may have facilitated immune cell activation before subsequent treatment cycles.

Taken together, these studies suggest that the principles articulated by Darragh and Karam—that radiation should precede immunotherapy to prime the immune system, that spacing fractions to allow T cell expansion is beneficial, and that the specific timing must be tailored to the mechanism of the immunotherapeutic agent—are highly relevant to the design of nucleic acid-loaded nanoradiosensitizers. Future development of these platforms should explicitly consider the immunological timing window, moving beyond simple co-administration toward rationally designed sequencing strategies that align with the kinetics of antigen release, dendritic cell activation, and T cell expansion. The integration of smart responsive nanoplatforms that can release their immunomodulatory payloads precisely during the window of peak immune activation, triggered by the radiation itself, represents a promising avenue for achieving this synchronization.

The timing of immune modulation relative to radiotherapy is increasingly recognized as a critical determinant of outcome. Deng and colleagues loaded PD-L1 siRNA into boron-containing polymer nanoparticles for boron neutron capture therapy (BNCT). As illustrated in Figure 4j, this approach not only sensitized tumors to BNCT but also downregulated intracellular PD-L1, which otherwise binds and stabilizes DNA repair mRNAs (BRCA1, MRE11, RAD50). The combination amplified DNA damage and immunogenic cell death while precisely killing tumor cells and sparing adjacent T cells, thereby inducing potent antitumor immunity against distal tumors [82]. This aligns with the principle that radiotherapy should first prime the immune system (by releasing antigens and DAMPs) before immune checkpoint inhibition is applied. Conversely, ATP-responsive hydrogels that release CpG only after radiotherapy-induced ATP peaks ensure that immune stimulation coincides with maximal antigen availability, rather than before [118]. A more sophisticated approach employs a metformin-based nanoplatform to deliver siTREX1 24 h before irradiation. This timing allows siTREX1 to downregulate the DNA exonuclease TREX1, preventing clearance of cytosolic DNA and thereby potentiating the cGAS-STING pathway

exactly when radiation produces DNA damage [119]. The lesson is clear: "when" the nucleic acid cargo is delivered may be as important as "what" and "where", and optimal schedules are mechanism-specific rather than universal.

5.6. STING-Targeted Signaling, lncRNAs, and Hematologic Malignancies

The immune-remodeling discussion should also include nucleic-acid-related innate sensing beyond CpG/TLR9. STING is activated by cyclic dinucleotides or cytosolic DNA-derived second messengers and functions downstream of cGAS, linking radiation-induced DNA damage to type I interferon signaling. Recent image-guided nanomedicine studies have used controlled delivery of STING agonists to create an immunologically hot tumor while limiting off-target inflammation; a pyridinium-rotor phototheranostic platform, for example, released the STING agonist MSA-2 under photothermal stimulation and induced type I interferon, abscopal suppression, and immune memory in triple-negative breast cancer models [121]. Although this example is not a nucleic acid nanocarrier in the strict sense, it highlights a pathway that can be integrated with CpG, siRNA, or ASO systems when radiation-induced cytosolic DNA is insufficient to sustain innate immune activation.

Immunoregulatory lncRNAs provide another layer of targetability. The present review already discusses lncMNX1-AS1 silencing as a means to reverse TNBC radioresistance [51], but translation is now beginning to move beyond preclinical proof-of-concept. A first-in-human phase I protocol is evaluating a TUG1-targeting ASO with a polymeric DDS for recurrent glioblastoma, based on the role of TUG1 in resolving R-loops and maintaining tumor growth [145]. Such examples suggest that lncRNAs may serve both as functional targets and as biomarkers for selecting patients whose radioresistance is driven by noncoding regulatory programs.

Most current nanoradio-immunotherapy work focuses on solid tumors, but hematologic malignancies offer important lessons because nodal or cutaneous lesions can be directly injected and monitored. In untreated indolent lymphoma, intratumoral SD-101, a class C CpG/TLR9 agonist, combined with local low-dose RT, induced regression of treated and untreated lesions with an acceptable safety profile [146]. These studies differ from systemic nanoparticle delivery in solid tumors, but they establish the clinical feasibility of coupling local irradiation with nucleic-acid immune adjuvants and provide a useful model for evaluating abscopal responses under more controlled clinical conditions.

6. Multimodal Joint Models: Beyond Additive Combination

6.1. Why Multimodal Design Is Emerging

Multimodal systems are now common because each component solves a different bottleneck. Radiation causes DNA damage but is limited by hypoxia and repair. High-Z materials increase local energy deposition but do not necessarily provide immune instruction. Nucleic acids can silence a target but require delivery precision. Immune adjuvants activate APCs but may need antigen release and checkpoint relief. Photothermal therapy can amplify ICD but is not inherently tumor-specific. Combining these functions can therefore be rational—if the sequence and biology are aligned.

6.2. Radiosensitization Plus Immunotherapy Plus Photothermal Therapy

Chen et al. provide an example of a truly integrated multimodal system [39]. Gold nanoflowers increased X-ray deposition, MnO_2 relieved hypoxia and enhanced ROS, PD-L1 aptamers improved specificity, BMS-202 blocked checkpoint signaling, and photothermal therapy amplified ICD. The resulting system induced substantial apoptosis, DNA damage, dendritic-cell maturation, T-cell activation, macrophage reprogramming, and abscopal control [39]. This is not simply a "combo" in the colloquial sense; it is a layered approach in which each component addresses a known failure mode of the others.

6.3. Radio-Immunotherapy Programmed by Biological Logic Gates

Ren et al.'s melanoma platform is distinctive because it introduces sequencing logic rather than mere co-delivery [38]. AUR first sensitizes melanoma cells to radiation and alters the tumor microenvironment. Radiation then increases ATP and MMP-2, which together trigger the release of a CpG-based adjuvant. In parallel, AUR suppresses VEGF-associated immunosuppressive recruitment. This is a strong prototype for future systems because it avoids indiscriminate simultaneous release. It uses the first therapeutic event to create the biochemical conditions for the second.

6.4. Local RT to Control Distant Immunosuppression

Zhang et al. proposed a different multimodal concept: use local RT not just to treat the primary tumor but to induce targetable immunosuppressive biology in distant tumors, then send a nucleic acid nanomedicine to those lesions [40]. Their iodine-containing cyanine dye enhanced RT locally, while CpG promoted immune activation. At the same time, RT-induced PD-L1 upregulation in distant tumors increased targeting of the PD-1-bearing fusion liposome, thereby reducing PD-L1 expression and MDSC function at distal sites [40]. This is an especially interesting strategy because it addresses a clinically relevant paradox: localized RT may generate both antitumor immune signals and systemic immunosuppressive consequences. A platform capable of exploiting the latter to reverse it is conceptually strong.

6.5. Ferroptosis-Centered Combinations

Ferroptosis is becoming a major theme in radiosensitization because radiation already perturbs redox balance and lipid peroxidation. Wang et al. combined iron delivery with silencing of a circular RNA that stabilized the SLC7A11/GPX4 ferroptosis defense machinery [136]. Ferroptosis has emerged as a major cell death pathway that can be exploited to overcome apoptosis resistance. Several studies have converged on the strategy of disrupting the SLC7A11/GSH/GPX4 antioxidant axis while simultaneously providing iron or iron-mimetic catalysts. A dual-channel radical amplifier (ATO@PAE-PEG-AS1411/Fe^{3+}) attacked this problem from two sides: atovaquone inhibited mitochondrial respiration to spare oxygen for ROS generation, while Fe^{3+} consumed GSH to preserve ROS, leading to a 2.5-fold reduction in tumor volume in a neuroblastoma model [101]. Another study used an FBXW7 DNAzyme-Fe^{2+} nanoassembly that not only stabilized p53 to induce G2 arrest but also transcriptionally suppressed SLC7A11, thereby crippling the cell's ferroptosis defense [48]. Interestingly, even nanoparticles not explicitly designed for ferroptosis may contribute to it: iron oxide-containing PIC nanoparticles likely release Fe ions that catalyze Fenton reactions, which may partially explain their strong immunomodulatory effects [120]. Collectively, these examples indicate that ferroptosis is not an alternative to apoptosis but a complementary pathway that can be activated by the same nucleic acid nanomedicines that also regulate cell cycle and immune checkpoints. Liu et al. used CRISPR-mediated disruption of GSS to reduce glutathione synthesis and inactivate GPX4 in glioblastoma [23]. These studies support an emerging model in which radiosensitization may be achieved not only by amplifying DNA damage but also by redirecting post-irradiation cell death mode toward ferroptosis. This may prove particularly relevant for tumors with apoptosis resistance.

6.6. When Multimodality Becomes Excessive

The main risk of multimodal design is that the system becomes too complex for reproducible manufacturing, dose control, safety evaluation, and regulatory approval. Each additional component introduces more variability: loading efficiency, release kinetics, immunogenicity, biodistribution, and drug-device interaction. Therefore, it needs a more disciplined standard for "necessary complexity". A useful rule is that each added component should solve a clearly identified biological bottleneck that cannot be addressed by a simpler formulation.

Comparison with conventional radiosensitizer classes also clarifies why programmable nucleic-acid nanomedicine is attractive. Small-molecule radiosensitizers such as PARP, ATR, ATM, or DNA-PK inhibitors have relatively defined pharmacology and easier manufacturing, but they often lack tumor-selective activation and can increase normal-tissue toxicity when paired with fractionated RT. Peptide-based delivery systems, including cell-penetrating peptides and peptide-protected gold nanoclusters, offer high uptake and sometimes favorable renal clearance, but their payload capacity, nuclease protection, and programmable logic are limited compared with modular nucleic acid nanocarriers [135,147]. Nucleic acid nanomedicine is therefore not a universal replacement; its value is highest when programmable target selection, immune instruction, or radiation-gated release is needed.

6.7. Emerging Radiation Modalities: Proton Therapy and FLASH Radiotherapy

The proposed four-dimensional framework can also be extended to advanced radiation modalities. Proton therapy offers spatial dose advantages through the Bragg peak, and therefore pairs naturally with nanomedicines designed to confine activation to a sharply defined volume. However, proton relative biological effectiveness, LET heterogeneity near the distal edge, and variable immune consequences mean that nanoparticle-radiation interactions should be measured under proton-specific conditions rather than extrapolated from photon data [139,148]. FLASH radiotherapy, delivered at ultra-high dose rates, may widen the therapeutic window through normal-tissue sparing, but its mechanisms remain incompletely resolved and may involve oxygen depletion, radical chemistry, and immune modulation [5,149]. For nucleic acid nanomedicine, FLASH raises a practical question: can carriers respond fast enough to exploit transient ROS, oxygen, and ATP changes generated over milliseconds to seconds? Future studies should directly compare conventional dose-rate RT, proton RT, and FLASH-like delivery using the same cargo, carrier, and tumor model before claiming modality-independent radiosensitization.

These translational considerations also point to broader design directions: multi-omics stratification and machine learning may help identify radiosensitization-relevant tumor subtypes, next-generation organic AIE nanoradiosensitizers and biomimetic organic nanozymes show how metal-free or metabolically responsive platforms can amplify ROS and antitumor immunity, and early clinical experience with liposome-encapsulated c-raf antisense oligodeoxyribonucleotide plus radiotherapy remains a reminder that nucleic-acid radiosensitizers must ultimately be evaluated under clinically realistic delivery and safety constraints [150–153].

7. Translational Challenges and Clinical Perspective

7.1. Model Systems Remain More Favorable Than the Clinic

Most studies in this field are still preclinical and use syngeneic or xenograft models with controlled timing, relatively uniform tumors, and idealized dosing schedules. Human tumors are more heterogeneous, particularly in vascularity, stromal density, checkpoint expression, and treatment history. Delivery systems that work well in small orthotopic murine tumors may face substantial dilution, sequestration, or immunological variability in patients.

Glioblastoma illustrates this clearly. Although BBB-penetrating and EV-based systems are promising, human BBB/BBTB heterogeneity, prior corticosteroid exposure, surgical cavities, and infiltrative margins pose major delivery challenges that are not fully captured in murine models [23,36].

7.2. Fractionation Matters

Many nanomedicine studies still use single-dose or simplified irradiation schedules. Yet clinical RT is usually fractionated, and fractionation shapes DNA repair, immune signaling, vascular response, and checkpoint dynamics [4,5,14]. Ren et al. appropriately examined dose and fractionation effects and found

that repeated 4 Gy schedules were superior to single low-dose exposure for their liposomal radio-immunotherapy platform [38]. This kind of design is likely to become more important. Radiosensitizers should be tested not only against radiation, but against clinical radiation logic.

7.3. Safety, Immunogenicity, and Off-Target Effects

Nucleic acid platforms must manage three different safety domains: carrier toxicity, nucleic acid toxicity, and combined radio-biological toxicity. For CRISPR systems, off-target editing remains a major concern, though Liu et al. reported low off-target frequencies and minimal systemic immunogenicity with their Ang/TAT-EV platform [23,36]. For immune adjuvants such as CpG, systemic cytokine activation and nonspecific immune effects require careful control. Logic-gated release, as in Ren et al., is attractive precisely because it minimizes premature leakage [38].

Materials matter as well. High-Z metals are effective but may raise long-term accumulation concerns. The move toward iodine-containing cyanine systems or biodegradable selenium-bridged silica reflects a growing awareness that radiosensitizer potency must be balanced against metabolic fate [36,40].

7.4. Manufacturing and Quality Control

The translational path for these systems will depend on reproducible synthesis, scale-up, batch consistency, sterility, shelf stability, and assayable critical quality attributes. Extracellular vesicles and membrane-camouflaged systems are biologically sophisticated but operationally challenging. Aptamer-modified liposomes and synthetic polymeric carriers may be easier to standardize, but can be less biologically adaptive. The eventual winners may be platforms that find the right compromise between biological intelligence and manufacturing discipline.

7.5. Biomarker-Guided Development

A major opportunity lies in biomarker-guided patient selection. Examples from the current field include high CFL1 expression, circADARB1 upregulation, GSS dependence, PD-L1 inducibility, LRP1 expression, and evidence of myeloid-dominant immune suppression [23,36,38–40,136]. Biomarker-driven patient selection is likely to determine which radiosensitizer succeeds in the clinic. Traditional tissue-based biomarkers (e.g., CFL1, circADARB1, GSS) are informative but static. Emerging functional imaging biomarkers offer real-time assessment of repair enzyme activity. At the transcriptomic level, a silver nanocluster-based radiosensitizer (NC-T5-5TR1) was found to exert its effect through the IL-6/JAK2/STAT3 axis; tumors with high baseline IL-6 expression were less responsive, suggesting that IL-6 could serve as an exclusion biomarker [131]. Together, these advances suggest that the future of nucleic acid-enabled radiosensitization lies in pairing each nanomedicine with a companion diagnostic—either a functional probe or a transcriptomic signature—to identify the patients most likely to benefit. Future clinical translation will likely require pairing each radiosensitizer with a biomarker strategy that identifies tumors most likely to respond. A programmable carrier is most valuable when paired with a rational biological indication.

8. Discussion

The central question in nucleic acid-enabled radiosensitization is no longer whether these systems can improve preclinical RT. They can. The more important question is what design principles are most likely to remain valid as the field moves toward clinical relevance.

First, precision delivery must be reframed as hierarchical control rather than a contest between passive and active targeting. The strongest platforms do not simply accumulate in tumors. They read successive layers of biological information: anatomical barriers, receptor expression, membrane behavior, intracellular

escape, and irradiation-induced chemistry. This layered precision is more meaningful than any single delivery mechanism considered in isolation.

Second, the strategic debate between a single attack and coordinated regulation should not be reduced to a numerical comparison of one target versus many. What matters is whether the intervention matches the organizational structure of radioresistance in a given tumor. In some cases, a dominant node such as GSS or circADARB1 may be sufficient because it governs a broad functional module [23,136]. In others, coordinated regulation is necessary because resistance is distributed across oxidative defense, checkpoint signaling, myeloid recruitment, and antigen presentation [38–40]. The optimal choice is therefore disease-specific and context-dependent.

Third, the concept of immune remodeling has matured. Early combination strategies emphasized relieving inhibition, especially PD-1/PD-L1 blockade. That remains important, but the current frontier lies in active immune instruction. CpG delivery, dendritic-cell programming, and logic-gated adjuvant release all reflect a deeper understanding of what irradiation alone cannot accomplish. This is a meaningful conceptual advance because it treats the immune system not merely as a downstream beneficiary of tumor cell death, but as a coequal therapeutic target.

Fourth, the most innovative systems now treat RT as a programmable context. Irradiation creates ROS, ATP gradients, protease changes, hypoxia shifts, and checkpoint induction. When nanomedicine is designed to respond to those conditions, RT becomes a spatially precise biological switch. This may be the most important idea to emerge from recent work. It suggests that future radiosensitizers should be designed not only to survive in the body, but to become fully active only in the irradiated state.

Fifth, complexity must be justified. The field has entered an era in which highly engineered systems are technically feasible, but not all complexity is translationally wise. A subtle but important tension exists within the field between minimal intelligence and maximal intelligence designs. Minimal-intelligence platforms—such as simple aptamer-gold nanoclusters—are easier to manufacture, scale, and regulate [125]. Their clinical translation path is shorter, but they may lack the adaptability to overcome complex, heterogeneous resistance mechanisms. Maximal-intelligence systems—such as AND-gated liposomes, DNA nanoclusters with logic-controlled release, or bacteriophage-based RNA scaffolds—achieve remarkable efficacy in animal models but pose significant challenges in batch consistency, stability, and regulatory approval [38,112,123]. A rational middle ground may be to design modular platforms where complexity is introduced only at specific bottlenecks. For example, the biodegradable gold supraccluster (BSC_gal) achieves high tumor accumulation and 90% clearance without an overly complex surface chemistry; its core innovation is the reversible crosslinker that responds to glutathione, not a dozen different functional moieties [129]. Similarly, the dual-targeted TfRA4-DNA1-Ag@Au nanoparticle uses two aptamers (one for BBB transcytosis, one for tumor targeting) but otherwise a straightforward core-shell structure, achieving enhanced glioma radiosensitization without exponential complexity [130]. The lesson is that complexity must be justified by a clear biological bottleneck, and every added layer should be tested for incremental benefit. Over-engineering may yield diminishing returns and hinder translation. A clinically credible platform must show that each functional layer contributes meaningful incremental benefit and does not merely decorate the formulation. In this regard, biology-guided complexity is preferable to technology-driven accumulation of features.

Several limitations of the current literature should also be acknowledged. Most studies remain in small-animal models, often using young mice, rapidly growing tumors, synchronized treatment timing, and short follow-up. Human tumors are more heterogeneous in vascular permeability, stromal density, immune history, microbiome exposure, and prior therapy. The majority of studies also lack direct comparison with clinically used radiosensitizers or with immunotherapy schedules used in patients. Long-term biodistribution and repeat-dose immunogenicity remain underexplored. Endpoint standardization is poor: some studies prioritize clonogenic survival, others apoptosis or immune infiltration, and only a minority

incorporate fractionation-relevant designs. Abscopal and memory effects should therefore be interpreted conservatively unless supported by untreated-lesion controls, rechallenge experiments, antigen-specific T-cell data, and immune-cell depletion or knockout validation.

Despite these limitations, the field is moving in a promising direction. The next phase will likely involve platforms that are somewhat simpler in construction but sharper in biological alignment: disease-specific targets, clinically relevant RT schedules, biomarker-linked patient selection, and more rigorous evaluation of systemic immune consequences. The true advance will not be one universal radiosensitizer, but a class of programmable radio-nucleic acid medicines tailored to distinct resistance ecologies.

9. Conclusions

Nucleic acid nanomedicine is redefining radiosensitization from a narrow effort to amplify DNA damage into a broader strategy of programmable tumor-state intervention. The most important recent advances are not limited to stronger nanoparticles or better cargo protection. They lie in the recognition that effective radiosensitization requires coordination across four dimensions: precise delivery, rational target architecture, purposeful immune remodeling, and biologically coherent multimodal integration.

Passive targeting remains useful, but active and conditional targeting now provide much greater therapeutic selectivity. Single-node interventions can be powerful when they disrupt major resistance modules, yet coordinated regulation often better matches the systems biology of radioresistant tumors. Immune remodeling has evolved from relieving inhibition to actively instructing dendritic cells, T cells, and myeloid compartments. Most importantly, RT is increasingly used as a spatial and temporal trigger that defines where and when the therapeutic system should become fully active.

The field's future will depend on moving from elegant proof-of-concept to clinically disciplined design: fractionation-aware studies, scalable manufacturing, safety by design, and biomarker-guided selection. With that shift, nucleic acid-enabled radiosensitization may become not merely an adjunct to RT, but a framework for integrating local irradiation with systemic and durable antitumor control.

Statement of the Use of Generative AI and AI-Assisted Technologies in the Writing Process

During the preparation of this manuscript, the authors used Deepseek in order to assist with language polishing and improving the clarity of the manuscript. After using this tool/service, the authors reviewed and edited the content as needed and take full responsibility for the content of the published article.

Acknowledgments

The authors would like to thank their colleagues for the insightful academic discussions and valuable suggestions, which greatly facilitated the conceptualization and drafting of this review. Schematic diagrams were generated in Adobe Illustrator.

Author Contributions

Conceptualization, C.L. and Y.X.; Writing—Original Draft Preparation, C.L., Y.Z. and N.J.; Writing—Review and Editing, C.L., X.M., C.S. and Y.X.; Figure Preparation, C.L.; Supervision, C.S. and Y.X.; Funding Acquisition, X.M. and Y.X. All authors have read and agreed to the published version of the manuscript.

Ethics Statement

Not applicable.

Informed Consent Statement

Not applicable.

Data Availability Statement

This is a Review article with no original data generated; all analyzed data are from previously published studies in the References with the permission of publisher.

Funding

This research was funded by the National Natural Science Foundation of China (Nos. 82373205, 82172661).

Declaration of Competing Interest

The authors declare that they have no known competing financial interests or personal relationships that could have appeared to influence the work reported in this paper.

References

1. Baskar R, Lee KA, Yeo R, Yeoh K-W. Cancer and radiation therapy: Current advances and future directions. *Int. J. Med. Sci.* **2012**, *9*, 193–199. DOI:10.7150/ijms.3635
2. Bazyar S, O'Brien ET, Benefield T, Roberts VR, Kumar RJ, Gupta GP, et al. Immune-mediated effects of microplanar radiotherapy with a small animal irradiator. *Cancers* **2021**, *14*, 155. DOI:10.3390/cancers14010155
3. Delaney G, Jacob S, Featherstone C, Barton M. The role of radiotherapy in cancer treatment: Estimating optimal utilization from a review of evidence-based clinical guidelines. *Cancer* **2005**, *104*, 1129–1137. DOI:10.1002/cncr.21324
4. Price JM, Prabhakaran A, West CML. Predicting tumour radiosensitivity to deliver precision radiotherapy. *Nat. Rev. Clin. Oncol.* **2023**, *20*, 83–98. DOI:10.1038/s41571-022-00709-y
5. Vozenin M-C, Bourhis J, Durante M. Towards clinical translation of FLASH radiotherapy. *Nat. Rev. Clin. Oncol.* **2022**, *19*, 791–803. DOI:10.1038/s41571-022-00697-z
6. Andratschke N, Willmann J, Appelt AL, Alyamani N, Balermpas P, Baumert BG, et al. European society for radiotherapy and oncology and european organisation for research and treatment of cancer consensus on re-irradiation: Definition, reporting, and clinical decision making. *Lancet Oncol.* **2022**, *23*, e469–e478. DOI:10.1016/S1470-2045(22)00447-8
7. Darragh LB, Gadwa J, Pham TT, Van Court B, Neupert B, Olimpo NA, et al. Elective nodal irradiation mitigates local and systemic immunity generated by combination radiation and immunotherapy in head and neck tumors. *Nat. Commun.* **2022**, *13*, 7015. DOI:10.1038/s41467-022-34676-w
8. Lei G, Zhang Y, Koppula P, Liu X, Zhang J, Lin SH, et al. The role of ferroptosis in ionizing radiation-induced cell death and tumor suppression. *Cell Res.* **2020**, *30*, 146–162. DOI:10.1038/s41422-019-0263-3
9. Lei G, Mao C, Yan Y, Zhuang L, Gan B. Ferroptosis, radiotherapy, and combination therapeutic strategies. *Protein Cell* **2021**, *12*, 836–857. DOI:10.1007/s13238-021-00841-y
10. Liu Y, Zheng C, Huang Y, He M, Xu WW, Li B. Molecular mechanisms of chemo- and radiotherapy resistance and the potential implications for cancer treatment. *MedComm* **2021**, *2*, 315–340. DOI:10.1002/mco2.55
11. Minniti G, Niyazi M, Alongi F, Navarria P, Belka C. Current status and recent advances in reirradiation of glioblastoma. *Radiat. Oncol.* **2021**, *16*, 36. DOI:10.1186/s13014-021-01767-9
12. Deng L, Liang H, Burnette B, Beckett M, Darga T, Weichselbaum RR, et al. Irradiation and anti–PD-L1 treatment synergistically promote antitumor immunity in mice. *J. Clin. Investig.* **2014**, *124*, 687–695. DOI:10.1172/JCI67313
13. Zhuang H. Abscopal effect of stereotactic radiotherapy combined with anti-PD-1/PD-L1 immunotherapy: Mechanisms, clinical efficacy, and issues. *Cancer Commun.* **2020**, *40*, 649–654. DOI:10.1002/cac2.12111
14. Gao Y, Li Y, Lin Z, Zeng Y, Huang Z, Han L, et al. Ataxia telangiectasia mutated kinase inhibition promotes irradiation-induced PD-L1 expression in tumour-associated macrophages through IFN-I/JAK signalling pathway. *Immunology* **2023**, *168*, 346–361. DOI:10.1111/imm.13602
15. James BR, Anderson KG, Brincks EL, Kucaba TA, Norian LA, Masopust D, et al. CpG-mediated modulation of MDSC contributes to the efficacy of Ad5-TRAIL therapy against renal cell carcinoma. *Cancer Immunol. Immunother.* **2014**, *63*, 1213–1227. DOI:10.1007/s00262-014-1598-8

16. Khilar S, Dembinska-Kenner A, Hall H, Syrmos N, Ligarotti GKI, Plaha P, et al. Towards a new dawn for neuro-oncology: Nanomedicine at the service of drug delivery for primary and secondary brain tumours. *Brain Sci.* **2025**, *15*, 136. DOI:10.3390/brainsci15020136
17. Ganau M, Foroni RI, Gerosa M, Longhi M, Nicolato A. Radiosurgical options in neuro-oncology: A review on current tenets and future opportunities. Part II: Adjuvant radiobiological tools. *Tumori* **2015**, *101*, 57–63. DOI:10.5301/tj.5000215
18. Zheng M, Tao W, Zou Y, Farokhzad OC, Shi B. Nanotechnology-based strategies for siRNA brain delivery for disease therapy. *Trends Biotechnol.* **2018**, *36*, 562–575. DOI:10.1016/j.tibtech.2018.01.006
19. Moss KH, Popova P, Hadrup SR, Astakhova K, Taskova M. Lipid nanoparticles for delivery of therapeutic RNA oligonucleotides. *Mol. Pharm.* **2019**, *16*, 2265–2277. DOI:10.1021/acs.molpharmaceut.8b01290
20. Kelly L, Maier KE, Yan A, Levy M. A comparative analysis of cell surface targeting aptamers. *Nat. Commun.* **2021**, *12*, 6275. DOI:10.1038/s41467-021-26463-w
21. Mohsen MG, Midy MK, Balaji A, Breaker RR. Exploiting natural riboswitches for aptamer engineering and validation. *Nucleic Acids Res.* **2023**, *51*, 966–981. DOI:10.1093/nar/gkac1218
22. Yang Y, Xu J, Sun Y, Mo L, Liu B, Pan X, et al. Aptamer-based logic computing reaction on living cells to enable non-antibody immune checkpoint blockade therapy. *J. Am. Chem. Soc.* **2021**, *143*, 8391–8401. DOI:10.1021/jacs.1c02016
23. Liu X, Cao Z, Wang W, Zou C, Wang Y, Pan L, et al. Engineered extracellular vesicle-delivered CRISPR/Cas9 for radiotherapy sensitization of glioblastoma. *ACS Nano* **2023**, *17*, 16432–16447. DOI:10.1021/acsnano.2c12857
24. Zhou H, Lu J, Yin B, Zhu Q, Chen Z. Achieving durable psoriasis remission with nucleic acid therapeutics. *Drug Discov. Today* **2026**, *31*, 104609. DOI:10.1016/j.drudis.2026.104609
25. Liu Q, Chen Y, Qi H. Advances in genotyping detection of fragmented nucleic acids. *Biosensors* **2024**, *14*, 465. DOI:10.3390/bios14100465
26. Wu S, Zhang Z, Zhao Z, Cui C, Tan W. Navigating the next frontier in biomedicine: Breakthroughs and insights in nucleic acid therapeutics. *Chem. Sci.* **2026**, *17*, 3377–3409. DOI:10.1039/d5sc06966a
27. Buzas EI. The roles of extracellular vesicles in the immune system. *Nat. Rev. Immunol.* **2023**, *23*, 236–250. DOI:10.1038/s41577-022-00763-8
28. Domingo-Espín J, Vázquez E, Ferrer-Miralles N, Corchero JL, Villaverde A. Engineered biological entities for drug delivery and gene therapy: Protein nanoparticles. *Prog. Mol. Biol. Transl. Sci.* **2011**, *104*, 247–298. DOI:10.1016/B978-0-12-416020-0.00006-1
29. Ying N, Liu S, Zhang M, Cheng J, Luo L, Jiang J, et al. Nano delivery system for paclitaxel: Recent advances in cancer theranostics. *Colloids Surf. B Biointerfaces* **2023**, *228*, 113419. DOI:10.1016/j.colsurfb.2023.113419
30. Yang X, Wang D, Li C, Zhang Y, Yang J, Liu M, et al. Nano-PROTACs for precision medicine: Engineering strategies for enhanced targeting and potency. *J. Nanobiotechnol.* **2026**, *24*, 120. DOI:10.1186/s12951-025-03985-9
31. Iqbal H, Razzaq A, Zhou D, Lou J, Xiao R, Lin F, et al. Nanomedicine in glaucoma treatment; Current challenges and future perspectives. *Mater. Today Bio* **2024**, *28*, 101229. DOI:10.1016/j.mtbio.2024.101229
32. Xu Z, Chi J, Qin F, Liu D, Lai Y, Bao Y, et al. Nanoparticles-incorporated hydrogel microneedle for biomedical applications: Fabrication strategies, emerging trends and future prospects. *Asian J. Pharm. Sci.* **2025**, *20*, 101069. DOI:10.1016/j.ajps.2025.101069
33. Jones T, Saba N. Nanotechnology and drug delivery: An update in oncology. *Pharmaceutics* **2011**, *3*, 171–185. DOI:10.3390/pharmaceutics3020171
34. Guo F, Luo S, Wang L, Wang M, Wu F, Wang Y, et al. Protein corona, influence on drug delivery system and its improvement strategy: A review. *Int. J. Biol. Macromol.* **2024**, *256*, 128513. DOI:10.1016/j.ijbiomac.2023.128513
35. Chen F, Cai W. Tumor vasculature targeting: A generally applicable approach for functionalized nanomaterials. *Small* **2014**, *10*, 1887–1893. DOI:10.1002/smll.201303627
36. Tang X, Wang Z, Xie Y, Liu Y, Yang K, Li T, et al. Radiation-triggered selenium-engineered mesoporous silica nanocapsules for RNAi therapy in radiotherapy-resistant glioblastoma. *ACS Nano* **2023**, *17*, 4062–4076. DOI:10.1021/acsnano.3c00269
37. Zou Y, Sun X, Yang Q, Zheng M, Shimoni O, Ruan W, et al. Blood-brain barrier–penetrating single CRISPR-Cas9 nanocapsules for effective and safe glioblastoma gene therapy. *Sci. Adv.* 2022, *8*, eabm8011. DOI:10.1126/sciadv.abm8011
38. Ren X, Xue R, Luo Y, Wang S, Ge X, Yao X, et al. Programmable melanoma-targeted radio-immunotherapy via fusogenic liposomes functionalized with multivariate-gated aptamer assemblies. *Nat. Commun.* **2024**, *15*, 5035. DOI:10.1038/s41467-024-49482-9
39. Chen B, He Y, Bai L, Pan S, Wang Y, Mu M, et al. Radiation-activated PD-L1 aptamer-functionalized nanoradiosensitizer to potentiate antitumor immunity in combined radioimmunotherapy and photothermal therapy. *J. Mater. Chem. B* **2024**, *12*, 12220–12231. DOI:10.1039/d4tb01831a

40. Zhang M, Gu L, Luo R, Liu D, Li J, Deng Z, et al. Nucleic acid/cyanine composite nanomedicine for targeted remote tumor therapy to counteract RT-induced immunosuppression. *Mater. Today* **2025**, *88*, 272–283. DOI:10.1016/j.mattod.2025.06.036
41. Liu M, Wang Y, Zhang Y, Hu D, Tang L, Zhou B, et al. Landscape of small nucleic acid therapeutics: Moving from the bench to the clinic as next-generation medicines. *Signal Transduct. Target. Ther.* **2025**, *10*, 73. DOI:10.1038/s41392-024-02112-8
42. Isenmann M, Stoddart MJ, Schmelzeisen R, Gross C, Della Bella E, Rothweiler RM. Basic principles of RNA interference: Nucleic acid types and in vitro intracellular delivery methods. *Micromachines* **2023**, *14*, 1321. DOI:10.3390/mi14071321
43. Yadav S, Van Vlerken LE, Little SR, Amiji MM. Evaluations of combination MDR-1 gene silencing and paclitaxel administration in biodegradable polymeric nanoparticle formulations to overcome multidrug resistance in cancer cells. *Cancer Chemother. Pharmacol.* **2009**, *63*, 711–722. DOI:10.1007/s00280-008-0790-y
44. Dunn SR, Phillips WS, Green DR, Weis VM. Knockdown of actin and caspase gene expression by RNA interference in the symbiotic anemone aiptasia pallida. *Biol. Bull.* **2007**, *212*, 250–258. DOI:10.2307/25066607
45. Wu W, Sun M, Zou G, Chen J. MicroRNA and cancer: Current status and prospective. *Int. J. Cancer* **2007**, *120*, 953–960. DOI:10.1002/ijc.22454
46. Fire A, Xu S, Montgomery MK, Kostas SA, Driver SE, Mello CC. Potent and specific genetic interference by double-stranded RNA in Caenorhabditis elegans. *Nature* **1998**, *391*, 806–811. DOI:10.1038/35888
47. Kievit FM, Wang K, Ozawa T, Tarudji AW, Silber JR, Holland EC, et al. Nanoparticle-mediated knockdown of DNA repair sensitizes cells to radiotherapy and extends survival in a genetic mouse model of glioblastoma. *Nanomedicine* **2017**, *13*, 2131–2139. DOI:10.1016/j.nano.2017.06.004
48. Yu J, Zhang Y, Li L, Xiang Y, Yao X, Zhao Y, et al. Coordination-driven FBXW7 DNAzyme-fe nanoassembly enables a binary switch of breast cancer cell cycle checkpoint responses for enhanced ferroptosis-radiotherapy. *Acta Biomater.* **2023**, *169*, 434–450. DOI:10.1016/j.actbio.2023.07.042
49. Vaughan HJ, Green JJ, Tzeng SY. Cancer-targeting nanoparticles for combinatorial nucleic acid delivery. *Adv. Mater.* **2020**, *32*, 1901081. DOI:10.1002/adma.201901081
50. Qiu C, Wu Y, Shi Q, Guo Q, Zhang J, Meng Y, et al. Advanced strategies for nucleic acids and small-molecular drugs in combined anticancer therapy. *Int. J. Biol. Sci.* **2023**, *19*, 789–810. DOI:10.7150/ijbs.79328
51. Yang Z, Shao B, Wang D, Chen H, Zhao X, Zeng M, et al. A TNBC-targeting nano-radiosensitizer reverses radioresistance by synergizing GSH scavenging with dual inhibition of Trop2 and lncRNA MNX1-AS1. *Biomaterials* **2026**, *327*, 123787. DOI:10.1016/j.biomaterials.2025.123787
52. Yu H-P, Liu F-C, Chung Y-K, Alalaiwe A, Sung CT, Fang J-Y. Nucleic acid-based nanotherapeutics for treating sepsis and associated organ injuries. *Theranostics* **2024**, *14*, 4411–4437. DOI:10.7150/thno.98487
53. Taina-González L, De La Fuente M. The potential of nanomedicine to unlock the limitless applications of mRNA. *Pharmaceutics* **2022**, *14*, 460. DOI:10.3390/pharmaceutics14020460
54. Edwards DK, Carfi A. Messenger ribonucleic acid vaccines against infectious diseases: Current concepts and future prospects. *Curr. Opin. Immunol.* **2022**, *77*, 102214. DOI:10.1016/j.coi.2022.102214
55. Sahin U, Karikó K, Türeci Ö. mRNA-based therapeutics—Developing a new class of drugs. *Nat. Rev. Drug Discov.* **2014**, *13*, 759–780. DOI:10.1038/nrd4278
56. Qin S, Tang X, Chen Y, Chen K, Fan N, Xiao W, et al. mRNA-based therapeutics: Powerful and versatile tools to combat diseases. *Signal Transduct. Target. Ther.* **2022**, *7*, 166. DOI:10.1038/s41392-022-01007-w
57. Ma Q, Zhang X, Yang J, Li H, Hao Y, Feng X. Optimization of the 5′ untranslated region of mRNA vaccines. *Sci. Rep.* **2024**, *14*, 19845. DOI:10.1038/s41598-024-70792-x
58. Zhang Z, Kuo JC-T, Yao S, Zhang C, Khan H, Lee RJ. CpG oligodeoxynucleotides for anticancer monotherapy from preclinical stages to clinical trials. *Pharmaceutics* **2021**, *14*, 73. DOI:10.3390/pharmaceutics14010073
59. Jordan M, Waxman DJ. CpG-1826 immunotherapy potentiates chemotherapeutic and anti-tumor immune responses to metronomic cyclophosphamide in a preclinical glioma model. *Cancer Lett.* **2016**, *373*, 88–96. DOI:10.1016/j.canlet.2015.11.029
60. Ma J, Fang Y, Hu J, Li S, Zeng L, Chen S, et al. Innovative microbial strategies in atopic dermatitis. *Front. Immunol.* **2025**, *16*, 1605434. DOI:10.3389/fimmu.2025.1605434
61. Sabatel C, Radermecker C, Fievez L, Paulissen G, Chakarov S, Fernandes C, et al. Exposure to bacterial CpG DNA protects from airway allergic inflammation by expanding regulatory lung interstitial macrophages. *Immunity* **2017**, *46*, 457–473. DOI:10.1016/j.immuni.2017.02.016
62. Vollmer J, Krieg AM. Immunotherapeutic applications of CpG oligodeoxynucleotide TLR9 agonists. *Adv. Drug Deliv. Rev.* **2009**, *61*, 195–204. DOI:10.1016/j.addr.2008.12.008

63. Bastian PJ, Yegnasubramanian S, Palapattu GS, Rogers CG, Lin X, De Marzo AM, et al. Molecular biomarker in prostate cancer: The role of CpG island hypermethylation. *Eur. Urol.* **2004**, *46*, 698–708. DOI:10.1016/j.eururo.2004.07.022
64. Manegold C, Gravenor D, Woytowitz D, Mezger J, Hirsh V, Albert G, et al. Randomized phase II trial of a toll-like receptor 9 agonist oligodeoxynucleotide, PF-3512676, in combination with first-line taxane plus platinum chemotherapy for advanced-stage non–small-cell lung cancer. *J. Clin. Oncol.* **2008**, *26*, 3979–3986. DOI:10.1200/JCO.2007.12.5807
65. Weber JS, Zarour H, Redman B, Trefzer U, O'Day S, Van Den Eertwegh AJM, et al. Randomized phase 2/3 trial of CpG oligodeoxynucleotide PF-3512676 alone or with dacarbazine for patients with unresectable stage III and IV melanoma. *Cancer* **2009**, *115*, 3944–3954. DOI:10.1002/cncr.24473
66. Yan Y, Liu S, Wen J, He Y, Duan C, Nabavi N, et al. Advances in RNA-based cancer therapeutics: Pre-clinical and clinical implications. *Mol. Cancer* **2025**, *24*, 251. DOI:10.1186/s12943-025-02463-y
67. Mayol B, Qubbaj IZ, Nava-Granados J, Vasquez K, Keene ST, Sempionatto JR. Aptamer and oligonucleotide-based biosensors for health applications. *Biosensors* **2025**, *15*, 277. DOI:10.3390/bios15050277
68. Sun H, Zu Y. Aptamers and their applications in nanomedicine. *Small* **2015**, *11*, 2352–2364. DOI:10.1002/smll.201403073
69. Meng H-M, Liu H, Kuai H, Peng R, Mo L, Zhang X-B. Aptamer-integrated DNA nanostructures for biosensing, bioimaging and cancer therapy. *Chem. Soc. Rev.* **2016**, *45*, 2583–2602. DOI:10.1039/c5cs00645g
70. Xiang D, Shigdar S, Qiao G, Zhou S-F, Li Y, Wei M, et al. Aptamer-mediated cancer gene therapy. *Curr. Gene Ther.* **2015**, *15*, 109–119. DOI:10.2174/1566523214666141224095105
71. Wong K-Y, Wong M-S, Lee JH, Liu J. From cell-SELEX to tissue-SELEX for targeted drug delivery and aptamer nanomedicine. *Adv. Drug Deliv. Rev.* **2025**, *224*, 115646. DOI:10.1016/j.addr.2025.115646
72. Yin S, Chen Z, Chen D, Yan D. Strategies targeting PD-L1 expression and associated opportunities for cancer combination therapy. *Theranostics* **2023**, *13*, 1520–1544. DOI:10.7150/thno.80091
73. Wu Y, Song Y, Wang R, Wang T. Molecular mechanisms of tumor resistance to radiotherapy. *Mol. Cancer* **2023**, *22*, 96. DOI:10.1186/s12943-023-01801-2
74. Drew Y, Zenke FT, Curtin NJ. DNA damage response inhibitors in cancer therapy: Lessons from the past, current status and future implications. *Nat. Rev. Drug Discov.* **2025**, *24*, 19–39. DOI:10.1038/s41573-024-01060-w
75. Huang R-X, Zhou P-K. DNA damage response signaling pathways and targets for radiotherapy sensitization in cancer. *Signal Transduct. Target. Ther.* **2020**, *5*, 60. DOI:10.1038/s41392-020-0150-x
76. Srinivas US, Tan BWQ, Vellayappan BA, Jeyasekharan AD. ROS and the DNA damage response in cancer. *Redox Biol.* **2019**, *25*, 101084. DOI:10.1016/j.redox.2018.101084
77. Groelly FJ, Fawkes M, Dagg RA, Blackford AN, Tarsounas M. Targeting DNA damage response pathways in cancer. *Nat. Rev. Cancer* **2023**, *23*, 78–94. DOI:10.1038/s41568-022-00535-5
78. Zhang W-W, Wright DG, Harrison L, Matlashewski G. Reconstitution of mycobacterium marinum nonhomologous DNA end joining pathway in leishmania. *mSphere* **2022**, *7*, e00156-22. DOI:10.1128/msphere.00156-22
79. Huang J. Reconstitution of the mammalian DNA double-strand break end-joining reaction reveals a requirement for an Mre11/Rad50/NBS1-containing fraction. *Nucleic Acids Res.* **2002**, *30*, 667–674. DOI:10.1093/nar/30.3.667
80. Syed A, Tainer JA. The MRE11–RAD50–NBS1 complex conducts the orchestration of damage signaling and outcomes to stress in DNA replication and repair. *Annu. Rev. Biochem.* **2018**, *87*, 263–294. DOI:10.1146/annurev-biochem-062917-012415
81. Zetrini AE, Abbasi AZ, He C, Lip H, Alradwan I, Rauth AM, et al. Targeting DNA damage repair mechanism by using RAD50-silencing siRNA nanoparticles to enhance radiotherapy in triple negative breast cancer. *Mater. Today Bio* **2024**, *28*, 101206. DOI:10.1016/j.mtbio.2024.101206
82. Deng S, Hu L, Chen G, Ye J, Xiao Z, Guan T, et al. A PD-L1 siRNA-loaded boron nanoparticle for targeted cancer radiotherapy and immunotherapy. *Adv. Mater.* **2025**, *37*, 2419418. DOI:10.1002/adma.202419418
83. Ngoi NYL, Peng G, Yap TA. A tale of two checkpoints: ATR inhibition and PD-(L)1 blockade. *Annu. Rev. Med.* **2022**, *73*, 231–250. DOI:10.1146/annurev-med-042320-025136
84. Yang Y, Duan Z, Liu X-L, Li Z, Shen Z, Gong S, et al. Checkpoint kinases regulate the circadian clock after DNA damage by influencing chromatin dynamics. *Nucleic Acids Res.* 2025, *53*, gkaf162. DOI:10.1093/nar/gkaf162
85. Shi C, Qin K, Lin A, Jiang A, Cheng Q, Liu Z, et al. The role of DNA damage repair (DDR) system in response to immune checkpoint inhibitor (ICI) therapy. *J. Exp. Clin. Cancer Res.* **2022**, *41*, 268. DOI:10.1186/s13046-022-02469-0
86. Fan J, Bellon M, Ju M, Zhao L, Wei M, Fu L, et al. Clinical significance of FBXW7 loss of function in human cancers. *Mol. Cancer* **2022**, *21*, 87. DOI:10.1186/s12943-022-01548-2
87. Mouw KW, Goldberg MS, Konstantinopoulos PA, D'Andrea AD. DNA damage and repair biomarkers of immunotherapy response. *Cancer Discov.* **2017**, *7*, 675–693. DOI:10.1158/2159-8290.CD-17-0226

88. Huang R, Zhou P-K. DNA damage repair: Historical perspectives, mechanistic pathways and clinical translation for targeted cancer therapy. *Signal Transduct. Target. Ther.* **2021**, *6*, 254. DOI:10.1038/s41392-021-00648-7
89. Niu X, You Q, Hou K, Tian Y, Wei P, Zhu Y, et al. Autophagy in cancer development, immune evasion, and drug resistance. *Drug Resist. Updat.* **2025**, *78*, 101170. DOI:10.1016/j.drup.2024.101170
90. Weiss F, Lauffenburger D, Friedl P. Towards targeting of shared mechanisms of cancer metastasis and therapy resistance. *Nat. Rev. Cancer* **2022**, *22*, 157–173. DOI:10.1038/s41568-021-00427-0
91. Liu Z, Ding Y, Ye N, Wild C, Chen H, Zhou J. Direct activation of bax protein for cancer therapy. *Med. Res. Rev.* **2016**, *36*, 313–341. DOI:10.1002/med.21379
92. Jackson MR, Ashton M, Koessinger AL, Dick C, Verheij M, Chalmers AJ. Mesothelioma cells depend on the antiapoptotic protein bcl-xL for survival and are sensitized to ionizing radiation by BH3-mimetics. *Int. J. Radiat. Oncol. Biol. Phys.* **2020**, *106*, 867–877. DOI:10.1016/j.ijrobp.2019.11.029
93. Condon LT, Ashman JNE, Ell SR, Stafford ND, Greenman J, Cawkwell L. Overexpression of bcl-2 in squamous cell carcinoma of the larynx: A marker of radioresistance. *Int. J. Cancer* **2002**, *100*, 472–475. DOI:10.1002/ijc.10503
94. Shu H-KG, Kim MM, Chen P, Furman F, Julin CM, Israel MA. The intrinsic radioresistance of glioblastoma-derived cell lines is associated with a failure of p53 to induce p21BAX expression. *Proc. Natl. Acad. Sci. USA* **1998**, *95*, 14453–14458. DOI:10.1073/pnas.95.24.14453
95. Chen X, Li J, Kang R, Klionsky DJ, Tang D. Ferroptosis: Machinery and regulation. *Autophagy* **2021**, *17*, 2054–2081. DOI:10.1080/15548627.2020.1810918
96. Chen F, Kang R, Tang D, Liu J. Ferroptosis: Principles and significance in health and disease. *J. Hematol. Oncol.* **2024**, *17*, 41. DOI:10.1186/s13045-024-01564-3
97. Bell HN, Stockwell BR, Zou W. Ironing out the role of ferroptosis in immunity. *Immunity* **2024**, *57*, 941–956. DOI:10.1016/j.immuni.2024.03.019
98. Lee SY, Jeong EK, Ju MK, Jeon HM, Kim MY, Kim CH, et al. Induction of metastasis, cancer stem cell phenotype, and oncogenic metabolism in cancer cells by ionizing radiation. *Mol. Cancer* **2017**, *16*, 10. DOI:10.1186/s12943-016-0577-4
99. Lei G, Zhang Y, Hong T, Zhang X, Liu X, Mao C, et al. Ferroptosis as a mechanism to mediate p53 function in tumor radiosensitivity. *Oncogene* **2021**, *40*, 3533–3547. DOI:10.1038/s41388-021-01790-w
100. Jiang L, Kon N, Li T, Wang S-J, Su T, Hibshoosh H, et al. Ferroptosis as a p53-mediated activity during tumour suppression. *Nature* **2015**, *520*, 57–62. DOI:10.1038/nature14344
101. Zhang W, Li X, Zeng J, Wen X, Zhang C, Zhang Y, et al. Enhancing the sensitization of neuroblastoma to radiotherapy by the construction of a dual-channel parallel free radicals nanoamplifier. *Mater. Today Bio* **2023**, *23*, 100828. DOI:10.1016/j.mtbio.2023.100828
102. Glaviano A, Lau HS-H, Carter LM, Lee EHC, Lam HY, Okina E, et al. Harnessing the tumor microenvironment: Targeted cancer therapies through modulation of epithelial-mesenchymal transition. *J. Hematol. Oncol.* **2025**, *18*, 6. DOI:10.1186/s13045-024-01634-6
103. Denk D, Greten FR. Inflammation: The incubator of the tumor microenvironment. *Trends Cancer* **2022**, *8*, 901–914. DOI:10.1016/j.trecan.2022.07.002
104. Liu J, Bai Y, Li Y, Li X, Luo K. Reprogramming the immunosuppressive tumor microenvironment through nanomedicine: An immunometabolism perspective. *eBioMedicine* **2024**, *107*, 105301. DOI:10.1016/j.ebiom.2024.105301
105. Pitt JM, Marabelle A, Eggermont A, Soria J-C, Kroemer G, Zitvogel L. Targeting the tumor microenvironment: Removing obstruction to anticancer immune responses and immunotherapy. *Ann. Oncol.* **2016**, *27*, 1482–1492. DOI:10.1093/annonc/mdw168
106. Tiwari A, Trivedi R, Lin S-Y. Tumor microenvironment: Barrier or opportunity towards effective cancer therapy. *J. Biomed. Sci.* **2022**, *29*, 83. DOI:10.1186/s12929-022-00866-3
107. Cowman SJ, Koh MY. Revisiting the HIF switch in the tumor and its immune microenvironment. *Trends Cancer* **2022**, *8*, 28–42. DOI:10.1016/j.trecan.2021.10.004
108. You L, Wu W, Wang X, Fang L, Adam V, Nepovimova E, et al. The role of hypoxia-inducible factor 1 in tumor immune evasion. *Med. Res. Rev.* **2021**, *41*, 1622–1643. DOI:10.1002/med.21771
109. Zhang F, Ma Y, Li D, Wei J, Chen K, Zhang E, et al. Cancer associated fibroblasts and metabolic reprogramming: Unraveling the intricate crosstalk in tumor evolution. *J. Hematol. Oncol.* **2024**, *17*, 80. DOI:10.1186/s13045-024-01600-2
110. Fang Z, Meng Q, Xu J, Wang W, Zhang B, Liu J, et al. Signaling pathways in cancer-associated fibroblasts: Recent advances and future perspectives. *Cancer Commun.* **2023**, *43*, 3–41. DOI:10.1002/cac2.12392
111. Qiu Z, Lu Z, Zhong Y, Li X, Zhang K, Li Z, et al. In situ genetically engineering nanosystem for reversing immunosuppression of cancer-associated fibroblasts in breast cancer radiotherapy. *Biomaterials* **2026**, *327*, 123795. DOI:10.1016/j.biomaterials.2025.123795

112. Xie Y, Li H, Xu L, Zou H, Wang X, He X, et al. DNA nanoclusters combined with one-shot radiotherapy augments cancer immunotherapy efficiency. *Adv. Mater.* **2023**, *35*, 2208546. DOI:10.1002/adma.202208546
113. Ma Y, Temkin SM, Hawkridge AM, Guo C, Wang W, Wang X-Y, et al. Fatty acid oxidation: An emerging facet of metabolic transformation in cancer. *Cancer Lett.* **2018**, *435*, 92–100. DOI:10.1016/j.canlet.2018.08.006
114. Jiang N, Xie B, Xiao W, Fan M, Xu S, Duan Y, et al. Fatty acid oxidation fuels glioblastoma radioresistance with CD47-mediated immune evasion. *Nat. Commun.* **2022**, *13*, 1511. DOI:10.1038/s41467-022-29137-3
115. Zhong Y, Chen X, Wu S, Fang H, Hong L, Shao L, et al. Deciphering colorectal cancer radioresistance and immune microrenvironment: Unraveling the role of EIF5A through single-cell RNA sequencing and machine learning. *Front. Immunol.* **2024**, *15*, 1466226. DOI:10.3389/fimmu.2024.1466226
116. Galassi C, Manic G, Esteller M, Galluzzi L, Vitale I. Epigenetic regulation of cancer stemness. *Signal Transduct. Target. Ther.* **2025**, *10*, 243. DOI:10.1038/s41392-025-02340-6
117. Kong YW, Dreaden EC, Morandell S, Zhou W, Dhara SS, Sriram G, et al. Enhancing chemotherapy response through augmented synthetic lethality by co-targeting nucleotide excision repair and cell-cycle checkpoints. *Nat. Commun.* **2020**, *11*, 4124. DOI:10.1038/s41467-020-17958-z
118. Sun L, Shen F, Tian L, Tao H, Xiong Z, Xu J, et al. ATP-responsive smart hydrogel releasing immune adjuvant synchronized with repeated chemotherapy or radiotherapy to boost antitumor immunity. *Adv. Mater.* **2021**, *33*, 2007910. DOI:10.1002/adma.202007910
119. He S, Huang Y, Liu J, Liu H, Chen Y, Zou T, et al. A metformin-based multifunctional nanoplatform as a DNA damage amplifier for maximized radio-immunotherapy to overcome radiotherapy resistance. *ACS Nano* **2025**, *19*, 14848–14864. DOI:10.1021/acsnano.4c18627
120. Zhang Y, Sriramaneni RN, Clark PA, Jagodinsky JC, Ye M, Jin W, et al. Multifunctional nanoparticle potentiates the in situ vaccination effect of radiation therapy and enhances response to immune checkpoint blockade. *Nat. Commun.* **2022**, *13*, 4948. DOI:10.1038/s41467-022-32645-x
121. Ning S, Shangguan P, Zhu X, Ou X, Wang K, Suo M, et al. Pyridinium rotor strategy toward a robust photothermal agent for STING activation and multimodal image-guided immunotherapy for triple-negative breast cancer. *J. Am. Chem. Soc.* **2025**, *147*, 7433–7444. DOI:10.1021/jacs.4c15534
122. Li D, Zhao J, Ma J, Yang H, Zhang X, Cao Y, et al. GMT8 aptamer conjugated PEGylated Ag@Au core-shell nanoparticles as a novel radiosensitizer for targeted radiotherapy of glioma. *Colloids Surf. B Biointerfaces* **2022**, *211*, 112330. DOI:10.1016/j.colsurfb.2022.112330
123. Pang H-H, Huang C-Y, Chen P-Y, Li N-S, Hsu Y-P, Wu J-K, et al. Bioengineered bacteriophage-like nanoparticles as RNAi therapeutics to enhance radiotherapy against glioblastomas. *ACS Nano* **2023**, *17*, 10407–10422. DOI:10.1021/acsnano.3c01102
124. Liu J, Guo L, Mi Z, Liu Z, Rong P, Zhou W. Vascular bursts-mediated tumor accumulation and deep penetration of spherical nucleic acids for synergistic radio-immunotherapy. *J. Control. Release* **2022**, *348*, 1050–1065. DOI:10.1016/j.jconrel.2022.06.030
125. Ghahremani F, Shahbazi-Gahrouei D, Kefayat A, Motaghi H, Mehrgardi MA, Javanmard SH. AS1411 aptamer conjugated gold nanoclusters as a targeted radiosensitizer for megavoltage radiation therapy of 4T1 breast cancer cells. *RSC Adv.* **2018**, *8*, 4249–4258. DOI:10.1039/c7ra11116a
126. Mehrnia SS, Hashemi B, Mowla SJ, Nikkhah M, Arbabi A. Radiosensitization of breast cancer cells using AS1411 aptamer-conjugated gold nanoparticles. *Radiat. Oncol.* **2021**, *16*, 33. DOI:10.1186/s13014-021-01751-3
127. Wang Z, Tang X, Zhao M, Zhang Y, Xiao Y, Liu Y, et al. Biomimetic hypoxia-triggered RNAi nanomedicine for synergistically mediating chemo/radiotherapy of glioblastoma. *J. Nanobiotechnol.* **2023**, *21*, 210. DOI:10.1186/s12951-023-01960-w
128. Yang Y, Liu B, Liu Y, Chen J, Sun Y, Pan X, et al. DNA-based MXFs to enhance radiotherapy and stimulate robust antitumor immune responses. *Nano Lett.* **2022**, *22*, 2826–2834. DOI:10.1021/acs.nanolett.1c04888
129. Jiang Y, Cao H, Deng H, Guan L, Langthasa J, Colburg DRC, et al. Gold-siRNA supraclusters enhance the anti-tumor immune response of stereotactic ablative radiotherapy at primary and metastatic tumors. *Nat. Biotechnol.* **2025**, *43*, 1496–1509. DOI:10.1038/s41587-024-02448-0
130. Kan X, Ma J, Ma J, Li D, Li F, Cao Y, et al. Dual-targeted TfRA4-DNA1-Ag@AuNPs: An innovative radiosensitizer for enhancing radiotherapy in glioblastoma multiforme. *Colloids Surf. B Biointerfaces* **2025**, *245*, 114328. DOI:10.1016/j.colsurfb.2024.114328
131. Kan X, Wang J, Li Y, Li D, Li F, Huang C, et al. Enhancing radiosensitization in triple-negative breast cancer by aptamer-modified nanoclusters NC-T5-5TR1. *Colloids Surf. B Biointerfaces* **2026**, *260*, 115397. DOI:10.1016/j.colsurfb.2025.115397

132. Zhang S, Gupta S, Fitzgerald TJ, Bogdanov AA. Dual radiosensitization and anti-STAT3 anti-proliferative strategy based on delivery of gold nanoparticle—Oligonucleotide nanoconstructs to head and neck cancer cells. *Nanotheranostics* **2018**, *2*, 1–11. DOI:10.7150/ntno.22335
133. Wei M, Shen X, Fan X, Li J, Bai J. PD-L1 aptamer-functionalized degradable hafnium oxide nanoparticles for near infrared-II diagnostic imaging and radiosensitization. *Front. Bioeng. Biotechnol.* **2023**, *11*, 1224339. DOI:10.3389/fbioe.2023.1224339
134. He J, Ren X, Zhang Q, Wang S, Li Z, Cai K, et al. Nanoradiosentizers with X ray-actuatable supramolecular aptamer building units for programmable immunostimulatory T cell engagement. *Biomaterials* **2025**, *315*, 122924. DOI:10.1016/j.biomaterials.2024.122924
135. Moro S, Omrani M, Erbek S, Jourdan M, Vandekerckhove CI, Nogier C, et al. Self-assembled peptide-gold nanoclusters with SiRNA targeting telomeric response to enhance radiosensitivity in lung cancer cells. *Small Sci.* **2025**, *5*, 2400156. DOI:10.1002/smsc.202400156
136. Wang D, Tang L, Chen M, Gong Z, Fan C, Qu H, et al. Nanocarriers targeting circular RNA ADARB1 boost radiosensitivity of nasopharyngeal carcinoma through synergically promoting ferroptosis. *ACS Nano* **2024**, *18*, 31055–31075. DOI:10.1021/acsnano.4c07676
137. Ranjan A, Jacobs GC, Woods DL, Negussie AH, Partanen A, Yarmolenko PS, et al. Image-guided drug delivery with magnetic resonance guided high intensity focused ultrasound and temperature sensitive liposomes in a rabbit Vx2 tumor model. *J. Control. Release* **2012**, *158*, 487–494. DOI:10.1016/j.jconrel.2011.12.011
138. Raj S, Khurana S, Choudhari R, Kesari KK, Kamal MA, Garg N, et al. Specific targeting cancer cells with nanoparticles and drug delivery in cancer therapy. *Semin. Cancer Biol.* **2021**, *69*, 166–177. DOI:10.1016/j.semcancer.2019.11.002
139. Liao Z, Lee JJ, Komaki R, Gomez DR, O'Reilly MS, Fossella FV, et al. Bayesian adaptive randomization trial of passive scattering proton therapy and intensity-modulated photon radiotherapy for locally advanced non–small-cell lung cancer. *J. Clin. Oncol.* **2018**, *36*, 1813–1822. DOI:10.1200/JCO.2017.74.0720
140. Subhan MA, Yalamarty SSK, Filipczak N, Parveen F, Torchilin VP. Recent advances in tumor targeting via EPR effect for cancer treatment. *J. Pers. Med.* **2021**, *11*, 571. DOI:10.3390/jpm11060571
141. Zhao F-Y, Shi L-Y, Yu L-J, Wang S-Q, Sun C-Y, Zhang N, et al. Decoding the ubiquitin network: Molecular mechanisms and therapeutic vulnerabilities for precision radio-sensitization in cancer. *Mol. Cancer* **2025**, *24*, 233. DOI:10.1186/s12943-025-02433-4
142. Aveic S, Tonini GP. Resistance to receptor tyrosine kinase inhibitors in solid tumors: Can we improve the cancer fighting strategy by blocking autophagy? *Cancer Cell Int.* **2016**, *16*, 62. DOI:10.1186/s12935-016-0341-2
143. Zhang Y, Gu Y, Zhan M, Yang L, Wang H. Targeting ferroptosis and cuproptosis in gastrointestinal cancers: Molecular mechanisms, metabolic vulnerabilities, and therapeutic interventions. *Mol. Biomed.* **2025**, *6*, 101. DOI:10.1186/s43556-025-00347-7
144. Darragh LB, Karam SD. Radiation as an immune modulator: Mechanisms and implications for combination with immunotherapy. *Nat. Rev. Cancer* 2026, 1–15. DOI:10.1038/s41568-025-00903-x
145. Deguchi S, Ohka F, Shiba Y, Yamaguchi J, Sato A, Shinjo K, et al. Investigator-initiated phase I trial of an oligonucleotide therapeutic targeting long noncoding RNA TUG1 for recurrent glioblastoma. *BMC Cancer* **2025**, *25*, 251. DOI:10.1186/s12885-025-13623-0
146. Frank MJ, Reagan PM, Bartlett NL, Gordon LI, Friedberg JW, Czerwinski DK, et al. In situ vaccination with a TLR9 agonist and local low-dose radiation induces systemic responses in untreated indolent lymphoma. *Cancer Discov.* **2018**, *8*, 1258–1269. DOI:10.1158/2159-8290.CD-18-0743
147. Roberts TC, Langer R, Wood MJA. Advances in oligonucleotide drug delivery. *Nat. Rev. Drug Discov.* **2020**, *19*, 673–694. DOI:10.1038/s41573-020-0075-7
148. Wang X, Zhang Y, Zhang X, Xiong Z, Xu K, Yue NJ, et al. Current advances in proton FLASH radiotherapy in abdominal cancers. *Cancers* **2026**, *18*, 758. DOI:10.3390/cancers18050758
149. Wang Y, Wang H, Hu J, Chai J, Luan J, Li J, et al. FLASH radiotherapy: Mechanisms, nanotherapeutic strategy and future development. *Nanoscale Adv.* **2025**, *7*, 711–721. DOI:10.1039/d4na00753k
150. Jiang Q, Yang A-Y, Mo G-L, Mo L-G, Deng T, Huang S-N, et al. Integrating multi-omics analysis and machine learning to refine molecular subtypes and prognostic assessment of lower-grade glioma. *Mol. Ther. Oncol.* **2026**, *34*, 201227. DOI:10.1016/j.omton.2026.201227
151. Xu Q, Zhang M, Huang Q, Gao S, Chu S, Li Q, et al. Organic AIE nanoradiosensitizer potentiates X-ray triggered continuous reactive oxygen species generation for potent cancer radioimmunotherapy. *Adv. Mater.* **2025**, *37*, e2502898. DOI:10.1002/adma.202502898

152. Suo M, Yang D, Yang M, Wang J, Zhang D, Zhu D, et al. Biomimetic organic nanozyme as tumor vaccines for targeted suppression of ammonia-induced T lymphocyte death to augment breast cancer immunotherapy. *Adv. Sci.* **2026**, *13*, e18037. DOI:10.1002/advs.202518037
153. Dritschilo A, Huang CH, Rudin CM, Marshall J, Collins B, Dul JL, et al. Phase I study of liposome-encapsulated c-raf antisense oligodeoxyribonucleotide infusion in combination with radiation therapy in patients with advanced malignancies. *Clin. Cancer Res.* **2006**, *12*, 1251–1259. DOI:10.1158/1078-0432.CCR-05-1260